*REVISED Manuscript (Clean version)
Click here to view linked References

Relationships between meteorological parameters and criteria air pollutants in three megacities in China

Hongliang Zhang[1], Yungang Wang[2,*], Jianlin Hu[3], Qi Ying[4], Xiao-Ming Hu[5]

[1]Department of Civil and Environmental Engineering, Louisiana State University, Baton Rouge, LA 70803, USA
[2]Environmental Resources Management (ERM), Walnut Creek, CA 94597, USA
[3]Department of Civil and Environmental Engineering, University of California, Davis, CA 95616, USA
[4]Zachry Department of Civil Engineering, Texas A&M University, College Station, TX 77843, USA
[5]Center for Analysis and Prediction of Storms, and School of Meteorology, University of Oklahoma, Norman, OK 73072, USA

*Corresponding author: Dr. Yungang Wang
Email: carl.wang@erm.com
Telephone: +1-925-946-0455

Abstract
Meteorological conditions play a crucial role in ambient air pollution by affecting both directly and indirectly the emissions, transport, formation, and deposition of air pollutants. In this study, the relationships between meteorological parameters and ambient air pollutants concentrations in three megacities in China, Beijing, Shanghai, and Guangzhou were investigated. A systematic analysis of air pollutants including $PM_{2.5}$, PM_{10}, CO, SO_2, NO_2, and O_3 and meteorological parameters including temperature, wind speed (WS), wind direction (WD) and relative humanity (RH) was conducted for a continuous period of 12 months from March 2013 to February 2014. The results show that all three cities experienced severe air quality problems. Clear seasonal trends were observed for $PM_{2.5}$, PM_{10}, CO, SO_2 and NO_2 with the maximum concentrations in the winter and the minimum in the summer, while O_3 exhibited an opposite trend. Substantially different correlations between air pollutants and meteorological parameters were observed among these three cities. WS reversely correlated with air pollutants, and temperature positively correlated with O_3. Easterly wind led to the highest $PM_{2.5}$ concentrations in Beijing, westerly wind led to high $PM_{2.5}$ concentrations in Shanghai, while northern wind blew air parcels with the highest $PM_{2.5}$ concentrations to Guangzhou. In Beijing, days of top 10 % $PM_{2.5}$, PM_{10}, CO, and NO_2 concentrations were with higher RH compared to days of bottom 10% concentrations, and SO_2 and O_3 showed no distinct RH dependencies. In Guangzhou, days of top 10 % $PM_{2.5}$, PM_{10}, CO, SO_2, NO_2 and O_3 concentrations were with lower RH compared to days of bottom 10% concentrations. Shanghai showed less fluctuation in RH between top and bottom 10%.
These results confirmed the important role of meteorological parameters in air pollution formation with large variations in different seasons and geological areas. These findings can be utilized to improve the understanding of the mechanisms that produce air pollution, enhance the forecast accuracy of the air pollution under different meteorological conditions, and provide effective measures for mitigating the pollution.

Keywords: Air pollution, Particulate matter, $PM_{2.5}$, China, Meteorology

1. Introduction

China holds rich culture and incredible history. Its large cities are transforming into cosmopolitan metropolises attracting enormous tourism, business development, and global integration. However, China's economic performance and growth over the last several decades can be overshadowed by the amount of air pollution the Chinese people inhale every day. In every major urban area across China, concentrations of air pollutants greatly exceed standards recommended by the World Health Organization (WHO).

Globally, 7 million deaths in 2012 were attributable to air pollution, which becomes the world's largest single environmental health risk accounting for one in eight of total global deaths (WHO, 2014). In China, between 350,000 and 500,000 people die prematurely each year as a result of outdoor air pollution, and it has become the fourth biggest threat to the health of Chinese people after heart disease, dietary risk and smoking (Chen et al., 2013a). The China's Huai River policy, which provides free winter heating via the provision of coal for boilers in cities north of the Huai River but denies heat to the south, leads to a reduction in life expectancies of 5.5 years (95% CI: 0.8, 10.2) in the north owing to an increased incidence of cardiorespiratory mortality (Chen et al., 2013b).

Previous air quality studies conducted in China mainly focus on the sources, the physical characteristics, and chemical composition of air pollutants (Cao et al., 2014; Wang et al., 2013a, Yuan et al., 2014). Several case studies have shown that meteorological conditions affect ambient air pollution in China in numerous ways. For example, Tian et al. (2014) reported that the air quality was the worst in spring, and got better in summer, subsequently tended to be more serious in autumn and winter in Beijing. Xu et al. (2011a) found that trace gas concentrations were strongly dependent on wind, and O_3 mixing ratio showed clear dependencies on temperature and relative humidity in North China Plain (NCP) region. Previous studies suggested that variation of the synoptic patterns modulated pollutant concentrations and likely provided the primary driving force for the day-to-day variations in the NCP regional pollution (Chen et al., 2008; Wang et al., 2009; Wei et al., 2011; Zhang et al., 2012a). Southerly/Southwesterly surface wind was found more likely to contribute to severe air pollution in the NCP (Wang et al., 2010; Wang et al., 2013b; Xu et al., 2011b). Results from Wang et al. (2014) showed that aerosol-radiation interactions played an important role in the haze episode in the NCP region. However, the knowledge gap between meteorological parameters and their impacts on concentrations of air pollutants remains wide.

In this study, a systematic analysis is presented to investigate the relationships of six criteria air pollutants ($PM_{2.5}$, PM_{10}, CO, SO_2, NO_2 and O_3) with meteorological parameters (wind direction, wind speed, temperature, and relative humidity) in three megacities based on a 12-month record of observations in 2013-2014. The goal is to unfold these vital relationships that can be utilized to improve the understanding of the mechanisms that produce air pollution, enhance the forecast accuracy of the air pollution under different meteorological conditions, and provide effective measures for mitigating the pollution.

2. Methods and data

2.1 Description of the study cities

Beijing, Shanghai, and Guangzhou were selected in this study. The locations of the three cities are shown in Figure 1. Beijing, Shanghai, and Guangzhou are located in the regions of NCP, the Yangtze River Delta (YRD), and the Pearl River Delta (PRD), respectively. The meteorological conditions in these three regions are substantially different. Moreover, these regions are hot spots of air pollution studies in China due to dense population, well developed economy, and frequent pollution events. Therefore, analyses of the data collected in these three cities could provide a broad and complete understanding on the relationships between meteorological parameters and criteria air pollutants in China.

Beijing, the capital of China with a population of 20.7 million in 2012 (http://www.stats.gov.cn/tjsj/ndsj/2013/indexeh.htm), is situated at the northern tip of the NCP region and is surrounded by mountains to the north, northwest, and west. Beijing has a monsoon-influenced continental climate, characterized by hot, humid summers, and cold, windy, and dry winters (Chen et al., 2007; Tian et al., 2014). Springs and falls are short and dry with sandstorms blowing in from Gobi Desert across the Mongolian steppe (Cao et al., 2014; Wang et al., 2014). Beijing is a key transportation hub with five ring roads, nine expressways, eleven national highways, ten conventional railways, and three high-speed railways converging in the city. In 2012, Beijing had approximately 5 million automobiles (http://www.stats.gov.cn/tjsj/ndsj/2013/indexch.htm).

Shanghai is the largest city by population in China with a population of 23.8 million in 2012 (http://www.stats.gov.cn/tjsj/ndsj/2013/indexeh.htm). Located at the mouth of the YRD region in East China, Shanghai is the world's busiest container port. Shanghai has a humid subtropical climate with cold and damp winter and hot and humid summer, susceptible to thunderstorms and typhoons (Bai et al., 2014; Xu et al., 2011a). Shanghai had more than 2 million automobiles in 2012 (http://www.stats.gov.cn/tjsj/ndsj/2013/indexch.htm).

Guangzhou is the provincial capital of Guangdong province and a representative mega-city in the PRD region in Southern China. It is a key national transportation hub and a major trading port. The city population was approximately 13 million in 2012 (http://www.gzstats.gov.cn/gzsq/). Guangzhou has a humid subtropical marine climate influenced by the East Asian monsoon, which spans from April to September (Li et al., 2014). With the rapid economic development over the past several decades, Guangzhou has experienced a rapid increase in the number of vehicles together with a substantial increase in biomass energy consumption (Huo et al., 2014).

2.2 Measurements and data analysis

Hourly meteorological parameters as well as concentrations of six criteria pollutants including $PM_{2.5}$, PM_{10}, CO, SO_2, NO_2 and O_3 in Beijing, Shanghai, and Guangzhou between March 2013 and February 2014 were included in this study. The surface meteorological data for each city, including temperature, wind speed, wind directions, and dew point were acquired from China Meteorological Administration in the Meteorological Information Comprehensive Analysis and Processing System (MICAPS) (Luo et al., 2006). Relative humidity was calculated using the temperature and dew point information. All the meteorological parameters have 8 measurements per day, conducted at local hour 02, 05, 08, 11, 14, 17, 20, and 23. Daily average meteorological parameters were then averaged using the 8 measurement results (scalar averaging for temperature and relative humidity, and vector averaging for wind speed and wind direction). All data from meteorological stations within a 20 km radius from the city center were included in the calculation of the city average meteorological parameters.

Measurements of the six criteria pollutants were conducted at the national air quality monitoring (AQM) sites. There are 13, 11, and 12 AQM sites located in Beijing, Shanghai, and Guangzhou, respectively. The data monitoring techniques have been described in a previous study (Hu et al., 2014), and therefore only a brief description is provided here. Automated monitoring systems were installed and used to measure the ambient concentration of SO_2, NO_2, O_3 and CO according to China Environmental Protection Standards HJ 193-2013 (http://www.es.org.cn/download/2013/7-12/2627-1.pdf), and of $PM_{2.5}$ and PM_{10} according to China Environmental Protection Standards HJ 655-2013 (http://www.es.org.cn/download/2013/7-12/2626-1.pdf).

The real-time hourly concentrations of $PM_{2.5}$, PM_{10}, CO, SO_2, NO_2, and O_3 were downloaded from the publishing website of the China National Environmental Monitoring Center (http://113.108.142.147:20035/emcpublish/). A sanity check was conducted on the hourly data at individual sites to remove problematic data points before calculating the average concentrations. The citywide average concentrations were calculated by averaging the concentrations at all sites in each city. The daily average meteorological parameters and pollutant concentrations were calculated only when there were valid data for more than 20 hours during that day.

Spearman-Rank correlation analysis was introduced to investigate the relationships between air pollutants and meteorological parameters (wind speed, temperature, and relative humidity). SigmaPlot (version 13) was used. The analysis was performed for each of the four seasons in each city independently. The 12 months are attributed to the following seasonal categories: spring (March, April, and May), summer (June, July, and August), fall (September, October, and November), and winter (December, January, and February). The wind direction categories are the following: $337.5^o < N \leq 22.5^o$, $22.5^o < NE \leq 67.5^o$, $67.5^o < E \leq 112.5^o$, $112.5^o < SE \leq 157.5^o$, $157.5^o < S \leq 202.5^o$, $202.5^o < SW \leq 247.5^o$, $247.5^o < W \leq 292.5^o$, $292.5^o < NW \leq 337.5^o$.

3 Results and discussions

3.1 Data overview

Table 1 shows the annual average, and minimum and maximum 24-hour average $PM_{2.5}$, PM_{10}, and gaseous species in Beijing, Shanghai, and Guangzhou during the entire study period. The annual averaged $PM_{2.5}$ concentrations in Beijing, Shanghai, and Guangzhou were 87.0, 56.1, and 51.6 μg/m^3, respectively, severely exceeding the Chinese Ambient Air Quality Standards (CAAQS) (15 μg/m^3 for Grade I and 35 μg/m^3 for Grade II). The maximum 24-hour average $PM_{2.5}$ concentrations were 391.6, 363.6, and 155.6 μg/m^3, respectively, indicating that extreme PM air pollution events happened in all the three cities. CO and SO_2 concentrations in Beijing were also the highest among the three while concentrations in Guangzhou were the lowest. NO_2 annual average concentrations in Beijing (25.4 ppb) and Guangzhou (24.4 ppb) were both approximately 20% higher than that in Shanghai (20.3 ppb). SO_2 and NO_2 concentrations in all three cities were equal to or exceeded the Grade I annual standards of CAAQS, which are ~7 ppb and ~21 ppb for SO_2 and NO_2, respectively. Guangzhou has the highest 1-h O_3, followed by Shanghai and Beijing, which is in comply with the geographical trend from south to north. 8-h O_3 had different trend compared to 1-h O_3, Shanghai had the largest value of 47.5 ppb and Guangzhou had the least value of 45.2 ppb.

Table 2 shows the annual statistical summary of meteorological parameters including wind speed (WS), ambient temperature (T), and relative humidity (RH). Beijing had the lowest annual average WS of 1.3 m/s but with the largest daily maximum of 5.9 m/s. Average WS in Shanghai and Guangzhou were close but Shanghai had lower daily maximum (4.6 m/s) than Guangzhou (5.7 m/s). Annual average T in Beijing, Shanghai, and Guangzhou were 13.7, 17.3, and 21.0 ^{o}C, respectively. Guangzhou had the highest annual average T but had the lowest daily maximum value. Guangzhou also had the highest annual RH of 78.0%, followed by Shanghai (68.0%) and Beijing (53.1%). In general, Beijing had the highest annual variability of daily averaged WS, T, and RH.

3.2 Temporal variations of air pollutants and meteorological variables

The annual analysis in the previous section provides an overview of the air pollutants in the three major metropolitan areas. As pollutants concentrations and meteorological conditions vary in different temporal scales, it is important to investigate their temporal variations before analyzing the relationship between them. Figure 2 shows the seasonal variations of all air pollutants. Average $PM_{2.5}$ concentrations in Beijing in all seasons were similar, and the highest concentration occurred in winter. Seasonal average $PM_{2.5}$ concentrations in Shanghai also peaked in winter, followed by spring, summer, and fall, successively. In Guangzhou, average $PM_{2.5}$ concentrations in summer (25 μg/m^3) were much lower than average concentrations in other seasons (~50 μg/m^3 in spring and fall and ~70 μg/m^3 in winter). PM_{10} has similar seasonal variation patterns as $PM_{2.5}$ in all cities.

CO concentrations in spring, summer, and fall were close in all three cities. CO concentrations in winter were higher than other three seasons with broader distribution. SO_2 concentrations in Beijing were highest in winter, followed by spring, and summer and fall, which had much lower concentrations. Similar results can be found in Shanghai but the differences between winter/spring and summer/fall were smaller. SO_2 concentrations in Guangzhou were comparable in all seasons but spring and winter had wider concentration ranges. NO_2 concentrations had similar seasonal distribution as SO_2 in all the three cities. Summer 1-h O_3 concentrations were highest in Beijing and Shanghai, followed by spring and fall. Winter time 1-h O_3 concentrations were generally much lower than those in other seasons. However, in Guangzhou 1-h O_3 concentration was highest in fall, and was comparable in other three seasons. 8-h O_3 concentrations had the same seasonal variation as the 1-h O_3 in all three cities. Generally, clear seasonal trends were observed for $PM_{2.5}$, PM_{10}, CO, SO_2 and NO_2 with the maximum in the winter and the minimum in the summer while 1-h O_3 and 8-h O_3 exhibited the opposite trend.

Seasonal variations of WS, T and RH are shown in Figure 3. In Beijing, WS was higher in spring and winter and lower in summer and fall. In Shanghai, WS gradually increased from 1.7 m/s in spring to 2.3 m/s in winter. In Guangzhou, WS were highest in winter (2.5 m/s), while lowest in summer (1.7 m/s). Averages of daily temperature in summer and winter in Beijing were highest and lowest, respectively, with very narrow ranges, while the values in spring and fall were very close except in spring the distribution was broader. Temperatures of Shanghai in all seasons were higher than in Beijing. In Guangzhou, the differences in temperature among seasons were smaller than in Beijing and Shanghai. Temperatures in summer days had very narrow range. In Beijing, summer and fall RH values were higher than in spring and winter. The highest RH values in summer had an average of 70%. In Shanghai and Guangzhou, RH values in all seasons were higher than in Beijing. Generally, RH had an increasing trend from spring to winter in Shanghai, while the trend was opposite in Guangzhou.

Seasonal distribution of wind direction at Beijing, Shanghai and Guangzhou are shown in Figure 4. In Beijing at spring, south wind was more frequent than north wind. However, north wind usually had larger speed. In summer, the WS was small and mostly from southwest. In fall, WS of south wind was small but that of northwest wind was large. In winter, south wind was much more frequent than north wind but the speed was much smaller. Wind in Shanghai was from all directions in all seasons. South wind was more frequent in spring and summer while north wind was more frequent in fall and winter. Southerly and northerly winds dominated wind direction in Guangzhou. In spring, north wind was slightly more frequent, while south wind was more frequent in summer. In fall and winter, north wind was prevalent, indicating the transport of pollutants from north may be important to Guangzhou.

Monthly variations of pollutants and meteorological parameters are shown in Figure S1 and Figure S2, respectively. All three regions showed diverse meteorological conditions, which gives us a good opportunity to study the relationships between air pollutants and meteorological variables in a very broad spectrum. Furthermore, the discussion of relationship between meteorological factors and pollutants is limited to seasonal variations to have enough data points for statistic calculations while keep the seasonal characteristics.

3.3 Correlation between air pollutants and WS, temperature and RH

The relationship between pollutants and meteorological factors was quantified using spearman-rank correlation coefficient as shown in Table 3. The correlations between all pollutants concentrations and the three meteorological parameters throughout the year were calculated. In Beijing, $PM_{2.5}$, PM_{10}, CO, SO_2, and NO_2 concentrations were negatively correlated with WS in all seasons except summer, which indicates horizontal dispersion plays important role in modulating their concentration in spring, fall, and winter. While in summer, vertical dispersion may play a more important role and horizontal dispersion plays a less important role when the atmospheric boundary layer can grow quite high (Table S1). The concentrations of $PM_{2.5}$, PM_{10}, CO, SO_2, and NO_2 positively correlated with RH in all seasons, especially in winter. High RH favors the partition of semi-volatile species into the aerosol phase (Hu et al., 2008), thus leading to high PM concentrations. Moister atmosphere normally accompanies lower boundary layer (Sandeep et al., 2014), thus further enhancing the concentrations of those primary source dominated pollutants. For the secondary pollutant of O_3, correlations with WS were negative in the summer and the fall, but positive in the winter. It is because high WS removes PM and increases the solar radiation, which enhances O_3 formation (Atkinson, 2000; Ran et al., 2009). The correlations with temperature were strongly positive in all seasons except for the winter, which is due to the significant role temperatures plays during O_3 formation (Jacob and Wineer, 2008; Rasmussen et al., 2012). The RH had negative correlations with O_3 in all seasons except for the fall.

In Shanghai, concentrations of all species except O_3 were negatively correlated with WS at all seasons. Like those in Beijing, O_3 concentrations in winter were positively correlated with WS. The highest correlations of O_3 with WS were found in summer. All pollutants, except O_3, were negatively correlated with temperature in spring and fall. The temperature correlation in summer and winter was weak. O_3 values were positively correlated with temperature with the highest correlation occurred in summer. In Shanghai, most pollutants, except CO in summer and O_3 in winter were negatively correlated with RH.

In Guangzhou, all air pollutants except with 8-h $O_3$was negatively correlated with WS in spring. Temperature positively related to $PM_{2.5}$, PM_{10}, SO_2, 1-h O_3, and 8-h O_3 in summer, and positively related all species in winter. In spring and fall, only weak negative correlations were observed. All pollutants except CO were negatively correlated with RH throughout the year.

The three cities showed similar correlation trends with different correlation coefficients between air pollutants and meteorological parameters. In general, higher WS was related with lower primary pollutants. For the secondary pollutant of O_3, higher concentrations are related with elevated temperatures.

3.4 Concentrations of pollutants as a function of wind directions

To better illustrate the effects of wind direction on pollutants. The concentrations of pollutants according to their respective wind directions were present. Figure 5 shows the results of $PM_{2.5}$ in Beijing, Shanghai, and Guangzhou. Easterly wind led to the highest $PM_{2.5}$ concentrations in Beijing followed by southerly wind. Northerly wind led to the lowest $PM_{2.5}$ concentrations. This is because northerly wind brings in relatively clean air from the mountains while the easterly and southerly wind transports pollutants from more polluted Tianjin and Central China (Ying et al., 2014; Zhang et al., 2012b). In Shanghai, the highest $PM_{2.5}$ concentrations were related to westerly wind followed by north wind, indicating the transport of pollutants from north and west to Shanghai had contributions to PM air pollution episodes in Shanghai (Ying et al., 2014). While in Guangzhou, northerly winds were associated with the highest $PM_{2.5}$ concentrations. Results of PM_{10}, CO, SO_2, NO_2, 1-h O_3 and 8-h O_3 according to their respective wind directions are shown in Figure S3. In generally, PM_{10} has similar results with $PM_{2.5}$. CO, SO_2, and NO_2, and high concentrations were related to easterly winds (including northeast, east, and southeast winds) in Beijing, westerly and northwesterly winds in Shanghai, and northerly and southeasterly winds in Guangzhou. 1-h O_3 and 8-h O_3 results are similar and their peak values are associated with southeasterly and southerly winds in Beijing, southerly and westerly winds in Shanghai, and northwesterly winds in Guangzhou.

The results clearly show that specific wind directions affect air pollutants more than other directions. This is likely due to two reasons. First, the emission intensities of pollutants and their precursors in the upwind areas of wind from the specific directions are larger compared to other areas. Thus, more pollutants were transported, which is considered as regional transport. The results are consistent with previous studies that have shown the importance of regional transport of pollutants and their precursors for all three cities (Cheng et al., 2014; Fan et al., 2014; Guo et al., 2014; Hu et al., 2014; Wang et al., 2014). Second, the speed of the wind coming from a specific direction is smaller compared to those from other directions, which is favorable for the accumulation of air pollutants. In the following section, the relationship of top 10% pollutant concentrations with wind speed is discussed.

3.5 Profiles of meteorological parameters under extreme air quality conditions

The top and bottom 10% concentrations of all pollutants are summarized in Table 4. It shows that the difference between top 10% and bottom 10% was apparent in all pollutants in all three regions. Figure 6 shows the top 10% and bottom 10% $PM_{2.5}$ associated together with WS and wind direction of the days when they occurred. In Beijing, the distribution of top 10% and bottom 10% $PM_{2.5}$, PM_{10}, CO, and NO_2 were generally identical. Top 10% was related with south and east winds at speeds lower than 2 m/s while bottom 10% was related with northerly wind at higher wind speed. SO_2, 1-h O_3 and 8-h O_3 were not different in top 10% and bottom 10%. In Shanghai, top 10% concentrations of $PM_{2.5}$, PM_{10}, CO, SO_2, and NO_2 were associated with west wind, indicating contributions from regional transport. Extreme 1-h O_3 and 8-h O_3 were associated with southerly wind with speeds less than 2 m/s. Bottom 10% $PM_{2.5}$, PM_{10}, CO, SO_2, and NO_2 were associated with wind from east and with speeds of 3-5 m/s while bottom 1-h O_3 and 8-h O_3 were related to north wind. In Guangzhou, top 10% concentrations of all pollutants were related with northerly wind, confirming that the importance of pollutants transport for severe pollution events. While bottom 10% concentrations were related to both north and south winds with higher wind speeds.

Figure 7 shows the comparison of temperature profiles between top 10% and bottom 10% daily pollutants in all three regions. When top 10% $PM_{2.5}$ concentrations happened, the temperatures were within -2 to 25 ˚C with an average of 8 ˚C. Bottom 10% $PM_{2.5}$ concentrations were observed when the temperature was between -5 and 30 ˚C with a higher average of 15 ˚C. In Shanghai, the difference between top 10% and bottom 10% were evident, top 10% happened more in lower temperature while bottom 10% happened in higher temperature, indicating that seasonal difference in $PM_{2.5}$ was important (see Figure 2). In Guangzhou, both top 10% and bottom 10% $PM_{2.5}$ concentrations occurred mostly in very narrow ranges centered at 15 to 25 ˚C, respectively. Temperature profiles of top and bottom PM_{10} in all three regions were similar to $PM_{2.5}$ but with less differences. Temperature profiles of top and bottom CO, SO_2, and NO_2 concentrations were also similar to $PM_{2.5}$ and PM_{10}, but the ranges and averages varied for different species and different regions. Temperature profiles of top 10% and bottom 10% 1-h O_3 and 8-h O_3 concentrations were much different from other pollutants. The top 10% O_3 concentrations happened on days with very high temperature while the bottom 10% concentrations usually happened on days with very low temperature. The difference in temperature was greater than 20 ˚C in Beijing and Shanghai, and less than 10 ˚C in Guangzhou.

Figure 8 shows the comparison of RH profiles between top 10% and bottom 10% concentrations of pollutants. In Beijing, the days of top 10% concentrations $PM_{2.5}$, PM_{10}, CO, and NO_2 were with 20% to 40% higher RH compared to the days of bottom 10% concentrations, and SO_2 and O_3 showed no distinct difference in RH. In Shanghai, it showed less fluctuation in RH between top and bottom 10%. Top 10% concentrations of pollutants happened on days with 5% to 15% lower RH than bottom 10% except for $PM_{2.5}$ and CO. In Guangzhou, the days of top 10% concentrations of all pollutants were with 5% to 20% lower RH compared to the days of bottom 10% concentrations.

All the surface meteorological parameters examined above are dictated by mesoscale/synoptic weather systems. It is meaningful for future air quality forecasting if all the meteorological parameters for the top and bottom 10% O_3 and $PM_{2.5}$ concentrations can be categorized into certain synoptic weather conditions. For the secondary pollutant of O_3, the formation depending heavily on temperature and radiation, the top 10% concentrations in all three cities occurred under the weather condition of strong radiation and thermal forcing (i.e., strong solar radiation and high temperature), while the bottom 10% concentrations were observed under weak radiation and thermal forcing.

For $PM_{2.5}$, contributed by both primary and secondary sources, it is hard to attribute all the favorable conditions for the top and bottom 10% concentrations into a single weather condition. In Beijing, the favorable conditions for the bottom 10% $PM_{2.5}$ concentrations include northerly wind, high temperature, and low RH. It is very unlikely to locate a weather system, which has all these conditions, because northerly wind is mostly associated with low temperature. In general, the $PM_{2.5}$ in the three cities is normally low under either strong synoptic forcing (e.g., windy days in spring) or strong thermal forcing (e.g., hot days in summer), while weak synoptic forcing and thermal forcing (e.g., calm and cold days in fall and winter) lead to high $PM_{2.5}$

concentrations. Considering the specific locations of emission sources around the three cities, in Beijing the top/bottom 10% $PM_{2.5}$ concentrations were found in the presence of southeasterly/northwesterly synoptic wind forcing. In Shanghai, the top/bottom 10% $PM_{2.5}$ concentrations were observed in the presence of westerly/easterly synoptic wind forcing. In Guangzhou, the top/bottom 10% $PM_{2.5}$ concentrations occurred in the presence of northerly/southerly synoptic wind forcing.

4 Conclusions

Our results show that all three megacities experienced severe air quality problems in the study episode with $PM_{2.5}$ concentrations higher than the CAAQS. In these three cities, clear seasonal trends were observed for $PM_{2.5}$, PM_{10}, CO, SO_2 and NO_2 with the maximum concentrations in the winter and the minimum in the summer. Such a seasonal variation was likely partially due to the seasonal variation of the atmospheric boundary layer (i.e., lower/higher boundary layer in winter/summer). The secondary pollutant of O_3 exhibited the opposite seasonal trend. Substantially different correlations between air pollutants and meteorological parameters were observed given the vastly different meteorological conditions. WS reversely correlated with air pollutants and O_3 positively related to temperature, indicating the important role of horizontal wind in pollutants dispersion and the important role of temperature in O_3-generating photochemical reactions. Easterly wind led to the highest $PM_{2.5}$ concentrations in Beijing, westerly wind led to the highest $PM_{2.5}$ concentrations in Shanghai, while northern wind blew air parcels with the highest $PM_{2.5}$ concentrations to Guangzhou. The differences in meteorological parameters between top 10% and bottom 10% concentrations of pollutants were also examined. Northerly winds were related to lower concentrations in Beijing, east winds led to lower concentrations in Shanghai, while south winds brought lower concentrations in Guangzhou. Top 10 % $PM_{2.5}$, PM_{10}, CO, SO_2, and NO_2 concentrations were related to lower wind speeds and lower temperature while O_3 concentrations were more related to higher temperature. Higher RH was associated with top 10% pollutants in Beijing but lower values in Guangzhou, while Shanghai showed less fluctuation in RH between top and bottom 10%.

This study generates important information for the role meteorological parameters play in the formation of air pollution. It provides a strong knowledge base for decision makers to implement effective air pollution control measures in China. It also implies that the impacts of global climate change on ambient air pollution and further on public health should be seriously considered. Although this study focused on the importance of surface meteorological variables on the atmospheric pollutants, vertical structure of the atmospheric boundary layer may also play important roles in modulating the surface pollutant concentrations (Hu et al., 2013, 2014; Hu, 2015; Klein et al., 2014; Haman et al., 2014). A following investigation of the impact of boundary layer structure on air pollutants in megacities is warranted once proper meteorological observations are available.

References

Atkinson, R., 2000. Atmospheric chemistry of VOCs and NOx, Atmos. Environ., 34, 2063-2101.

Bai, L., Ding, G., Gu, S., Bi, P., Su, B., Qin, D., Xu, G., Liu, Q., 2014. The effects of summer temperature and heat waves on heat-related illness in a coastal city of China, 2011-2013. Environ. Res. 132, 212-219.

Cao, C., Zheng, S., Singh, R., 2014. Characteristics of aerosol optical properties and meteorological parameters during three major dust events (2005–2010) over Beijing, China. Atmos. Res. 150, 129-142.

Chen, D., Cheng, S., Liu, L., Chen, T., Guo, X., 2007. An integrated MM5-CMAQ modeling approach for assessing trans-boundary PM_{10} contribution to the host city of 2008 Olympic summer games-Beijing, China. Atmos. Environ. 41, 1237-1250.

Chen, Z. H., S. Y. Cheng, J. B. Li, X. R. Guo, W. H. Wang, and D. S. Chen, 2008, Relationship between atmospheric pollution processes and synoptic pressure patterns in northern China, *Atmos Environ*, *42*(24), 6078-6087, DOI 10.1016/j.atmosenv.2008.03.043.

Chen, Z., Wang, J., Ma, G., Zhang, Y., 2013a. China Tackles the Health Effects of Air Pollution. Lancet 382, 1959-1960.

Chen, Y., Ebenstein, A., Greenstone, M., Li, H., 2013b. Evidence on the impact of sustained exposure to air pollution on life expectancy from China's Huai River policy. Proc. Natl. Acad. Sci. USA 110, 12936–12941.

Cheng, Z., Wang, S., Fu, X., Watson, J., Jiang, J., Fu, Q., Chen, C., Xu, B., Yu, J., Chow, J., Hao, J., 2014. Impact of biomass burning on haze pollution in the Yangtze River delta, China: a case study in summer 2011. Atmos. Chem. Phys. 14, 4573-4585.Fan, Q., Yu, W., Fan, S., Wang, X., Lan, J., Zou, D., Feng, Y., Chan, P., 2014. Process analysis of a regional air pollution episode over Pearl River Delta Region, China, using the MM5-CMAQ model. J. Air Waste Manag. Assoc. 64, 406-418.

Guo, S., Hu, M., Zamora, M., Peng, J., Shang, D., Zheng, J., Du, Z., Wu, Z., Shao, M., Zeng, L., Molina, M., Zhang, R., 2014. Elucidating severe urban haze formation in China. Proc. Natl. Acad. Sci. USA 111, 17373-17378.

Haman, C. L., E. Couzo, J. H. Flynn, W. Vizuete, B. Heffron, *and* B. L. Lefer (2014), Relationship between boundary layer heights and growth rates with ground-level ozone in Houston, Texas, J. Geophys. Res. Atmos., 119, 6230–6245. doi:10.1002/2013JD020473.

Hu, X.-M., Y. Zhang, M. Z. Jacobson, and C. K. Chan (2008), Coupling and evaluating gas/particle mass transfer treatments for aerosol simulation and forecast, J. Geophys. Res., 113, D11208, doi:10.1029/2007JD009588.

Hu, X.-M., P. Klein , M. Xue, F. Zhang, D. Doughty, R. Forkel, E. Joseph, and J. D. Fuentes (2013), Impact of the Vertical Mixing Induced by Low-level Jets on Boundary Layer Ozone Concentration, *Atmos. Environ.*, 70, 123-130

Hu, X. M., Z. Q. Ma, W. L. Lin, H. L. Zhang, J. L. Hu, Y. Wang, X. B. Xu, J. D. Fuentes, and M. Xue (2014), Impact of the Loess Plateau on the atmospheric boundary layer structure and air quality in the North China Plain: A case study, Sci Total Environ, 499, 228-237. doi: 10.1016/j.scitotenv.2014.08.053.

Hu, X. M. (2015), BOUNDARY LAYER (ATMOSPHERIC) AND AIR POLLUTION | Air Pollution Meteorology, in *Encyclopedia of Atmospheric Sciences (Second Edition)*, edited by G. R. North, J.

Pyle and F. Zhang, pp. 227-236, Academic Press, Oxford. http://dx.doi.org/10.1016/B978-0-12-382225-3.00499-0.

Hu, J., Wang, Y., Ying, Q., Zhang, H., 2014. Spatial and temporal variability of $PM_{2.5}$ and PM_{10} over the North China Plain and the Yangtze River Delta, China. Atmos. Environ. 95, 598-609.

Huo, H., Zheng, B., Wang, M., Zhang, Q., He, K., 2014. Vehicular air pollutant emissions in China: evaluation of past control policies and future perspectives. Mitigation and Adaptation Strategies for Global Change. doi: 10.1007/s11027-014-9613-0.

Jacob, D. J., D. A. Winner, 2009. Effect of climate change on air quality. Atmospheric Environment. 43, 51-63, DOI:10.1016/j.atmosenv.2008.09.051.

Klein, P. M., X.-M. Hu, M. Xue (2014), Mixing processes in the nocturnal atmospheric boundary layer and their impacts on urban ozone concentrations, *Bound.-layer meteor.*, doi:10.1007/s10546-013-9864-4.

Li, L., Qian, J., Ou, C., Zhou, Y., Guo, C., Guo, Y., 2014. Spatial and temporal analysis of Air Pollution Index and its timescale-dependent relationship with meteorological factors in Guangzhou, China, 2001-2011. Environ. Pollu. 190, 75-81.

Luo, B., X. Tan and Y. Guo, 2006, Introduction of MICAPS - A Chinese Forecaster's Interactive System, presentation at the 86^{th} AMS Annual Meeting/the 8^{th} Conference on atmospheric chemistry, 27 Jan.–3 Feb., Atlanta, GA. https://ams.confex.com/ams/pdfpapers/98266.pdf

Ran, L., C. Zhao, F. Geng, X. Tie, X. Tang, L. Peng, G. Zhou, Q. Yu, J. Xu, and A. Guenther, (2009). Ozone photochemical production in urban Shanghai, China: Analysis based on ground level observations, J. Geophys. Res., 114, D15301, doi:10.1029/2008JD010752.

Rasmussen, D.J., A.M. Fiore, V. Naik, L.W. Horowitz, S.J. McGinnis, M.G. Schultz, 2012. Surface ozone-temperature relationships in the eastern US: A monthly climatology for evaluating chemistry-climate models. Atmospheric Environment, 47, 142-153. DOI. 10.1016/j.atmosenv.2011.11.021.

Sandeep, A,. Rao, T.N., Ramkiran, C.N., Rao, S.V.B., 2014. Differences in atmospheric boundary-layer characteristics between wet and dry episodes of the Indian summer monsoon. Bound-Lay Meteorol, 1–20. http://dx.doi.org/10.1007/s10546-014-9945-z.

Tian, G., Qiao, Z., Xu, X., 2014. Characteristics of particulate matter (PM_{10}) and its relationship with meteorological factors during 2001-2012 in Beijing. Environ. Pollu. 192, 266-274.

Wang, Y., J. Hao, M. B. McElroy, J. W. Munger, H. Ma, D. Chen, and C. P. Nielsen, 2009. Ozone air quality during the 2008 Beijing Olympics: effectiveness of emission restrictions, *Atmos Chem Phys*, *9* (14), 5237-5251.

Wang, F., D. S. Chen, S. Y. Cheng, J. B. Li, M. J. Li, and Z. H. Ren, 2010. Identification of regional atmospheric PM_{10} transport pathways using HYSPLIT, MM5-CMAQ and synoptic pressure pattern analysis, *Environ Modell Softw*, *25*(8), 927-934, DOI 10.1016/j.envsoft.2010.02.004.

Wang, J., Hu, Z., Chen, Y., Chen, Z., Xu, S., 2013a. Contamination characteristics and possible sources of PM_{10} and $PM_{2.5}$ in different functional areas of Shanghai, China. Atmos. Environ. 68, 221-229.

Wang, Z. B., M. Hu, Z. J. Wu, D. L. Yue, L. Y. He, X. F. Huang, X. G. Liu, and A. Wiedensohler, 2013b. Long-term measurements of particle number size distributions and the relationships with air mass history and source apportionment in the summer of Beijing, *Atmos Chem Phys*, *13*(20), 10159-10170, DOI 10.5194/acp-13-10159-2013.

Wang, R., Zou, X., Cheng, H., Wu, Z., Zhang, C., Kang, L., 2014. Spatial distribution and source apportionment of atmospheric dust fall at Beijing during spring of 2008-2009. Environ. Sci. Pollut. Res. Int. doi: 10.1007/s11356-014-3583-3.

Wei, P., S. Y. Cheng, J. B. Li, and F. Q. Su (2011), Impact of boundary-layer anticyclonic weather system on regional air quality, *Atmos Environ*, *45*(14), 2453-2463, DOI 10.1016/j.atmosenv.2011.01.045.

World Health Organization (WHO), 2014. Burden of disease from the joint effects of Household and Ambient Air Pollution for 2012. http://www.who.int/phe/health_topics/outdoorair/databases/FINAL_HAP_AAP_BoD_24March2014.pdf?ua=1 (Accessed on January 2, 2015)

Xu, W., Zhao, C., Ran, L., Deng, Z., Liu, P., Ma, N., Lin, W., Xu, X., Yan, P., He, X., Yu, J., Liang, W., Chen, L., 2011a. Characteristics of pollutants and their correlation to meteorological conditions at a suburban site in the North China Plain. Atmos. Chem. Phys. 11, 4353-4369.

Xu, J., J. Z. Ma, X. L. Zhang, X. B. Xu, X. F. Xu, W. L. Lin, Y. Wang, W. Meng, and Z. Q. Ma (2011b), Measurements of ozone and its precursors in Beijing during summertime: impact of urban plumes on ozone pollution in downwind rural areas, *Atmos Chem Phys*, *11*(23), 12241-12252, DOI 10.5194/acp-11-12241-2011.

Xue, L., Wang, T., Gao, J., Ding, A., Zhou, X., Blake, D., Wang, X., Saunders, S., Fan, S., Zuo, H., Zhang, Q., Wang, W., 2014. Ground-level ozone in four Chinese cities: precursors, regional transport and heterogeneous processes. Atmos. Chem. Phys. 14, 13175-13188.

Ying, Q., Wu, L., Zhang, H., 2014. Local and inter-regional contributions to $PM_{2.5}$ nitrate and sulfate in China. Atmos. Environ. 94, 582-592.

Yuan, Q., Yang, L., Dong, C., Yan, C., Meng, C., Sui, X., Wang, W., 2014. Particle physical characterization in the Yellow River Delta of Eastern China: number size distribution and new particle formation. doi: 10.1007/s11869-014-0293-4.

Zhang, J. P., et al. (2012a), The impact of circulation patterns on regional transport pathways and air quality over Beijing and its surroundings, *Atmos Chem Phys*, *12*(11), 5031-5053, DOI 10.5194/acp-12-5031-2012.

Zhang, H., Li, J., Ying, Q., Yu, J., Wu, D., Cheng, Y., He, K., Jiang, J., 2012b. Source apportionment of $PM_{2.5}$ nitrate and sulfate in China using a source-oriented chemical transport model. Atmos. Environ. 62, 228-242.

Table 1. Statistical summary of the daily average concentrations of $PM_{2.5}$, PM_{10}, and gaseous pollutant concentrations during the entire sampling period (March 2013 – February 2014). Units: µg/m^3 for $PM_{2.5}$ and PM_{10}; ppb for all other gaseous pollutants.

		$PM_{2.5}$	**PM_{10}**	**CO**	**SO_2**	**NO_2**	**1-h O_3**	**8-h O_3**
Beijing	Average	87.0	109.4	1068.4	8.6	25.4	52.5	45.3
	Min	5.4	14.6	228.8	0.7	4.1	4.3	2.7
	Median	66.7	96.8	869.6	5.1	22.6	42.6	41.5
	Max	391.6	408.8	3882.5	45.7	66.6	143.7	114.6
	Count	342	311	326	332	331	303	303
Shanghai	Average	56.1	79.9	703.9	7.3	20.3	56.1	47.5
	Min	6.2	22.5	337.7	2.1	3.3	15.8	11.0
	Median	45.3	64.0	639.4	5.6	18.4	50.1	44.2
	Max	363.4	291.1	2152.4	27.3	53.2	149.9	123.3
	Count	339	311	321	332	332	327	327
Guangzhou	Average	51.6	72.5	820.7	7.2	24.4	58.3	45.2
	Min	8.3	19.1	484.5	1.1	8.4	9.7	7.0
	Median	46.7	66.9	782.4	6.7	22.1	55.4	42.4
	Max	155.6	192.7	2101.9	19.7	60.5	139.4	134.0
	Count	320	321	305	313	313	306	306

Note: The maximum concentrations of $PM_{2.5}$ and PM_{10} were not observed on the same day.

Table 2. Statistical summary for the daily average measurements of surface wind speed (WS, m/s), ambient temperature (T, ^{o}C), and relative humidity (RH, %).

		WS	**T**	**RH**
Beijing	Average	1.3	13.7	53.1
	Min	0.0	-5.5	11.6
	Median	1.1	13.2	52.1
	Max	5.9	32.3	97.3
	Count	358	358	358
Shanghai	Average	2.0	17.3	68.0
	Min	0.2	-0.3	34.5
	Median	1.9	18.4	68.0
	Max	4.6	35.4	98.3
	Count	362	362	362
Guangzhou	Average	2.1	21.0	78.0
	Min	0.1	4.9	29.4
	Median	1.8	22.7	79.3
	Max	5.7	30.8	98.3
	Count	362	362	362

Table 3. Summary of Spearman-Rank correlation coefficient values. Numbers highlighted in green indicate negative correlation, while numbers highlighted in orange indicate positive correlation. The darker the color, the stronger the correlation.

Beijing

		$PM_{2.5}$	PM_{10}	CO	SO_2	NO_2	1-h O_3	8-h O_3
WS	Spring	-0.24	-0.16	-0.35	-0.33	-0.38	0.02	0.00
	Summer	0.16	0.16	0.18	0.23	-0.05	-0.17	-0.08
	Fall	-0.37	-0.30	-0.42	-0.22	-0.43	-0.16	-0.15
	Winter	-0.25	-0.25	-0.33	-0.35	-0.40	0.37	0.41
Temp	Spring	-0.03	0.21	-0.27	-0.11	-0.12	0.72	0.71
	Summer	-0.26	-0.06	-0.39	-0.06	-0.34	0.54	0.42
	Fall	0.01	0.01	-0.04	-0.37	-0.19	0.66	0.74
	Winter	0.12	0.15	0.09	-0.03	-0.01	0.16	0.08
RH	Spring	0.65	0.41	0.55	0.34	0.36	-0.18	-0.13
	Summer	0.52	0.09	0.59	-0.09	0.18	-0.43	-0.33
	Fall	0.66	0.47	0.59	0.14	0.46	0.25	0.23
	Winter	0.86	0.77	0.75	0.68	0.68	-0.54	-0.58

Shanghai

		$PM_{2.5}$	PM_{10}	CO	SO_2	NO_2	1-h O_3	8-h O_3
WS	Spring	-0.45	-0.39	-0.50	-0.47	-0.53	-0.13	-0.13
	Summer	-0.68	-0.58	-0.54	-0.46	-0.65	-0.53	-0.46
	Fall	-0.29	-0.17	-0.26	-0.32	-0.55	-0.23	-0.01
	Winter	-0.38	-0.28	-0.40	-0.31	-0.62	0.09	0.24
Temp	Spring	-0.03	-0.16	-0.15	-0.21	-0.22	0.13	0.01
	Summer	0.10	0.39	-0.19	0.45	0.03	0.60	0.61
	Fall	-0.54	-0.64	-0.57	-0.70	-0.58	0.13	0.22
	Winter	0.18	0.12	0.04	-0.21	0.14	0.44	0.29
RH	Spring	-0.26	-0.33	-0.04	-0.47	-0.25	-0.69	-0.66
	Summer	-0.09	-0.34	0.22	-0.47	-0.02	-0.56	-0.60
	Fall	0.06	-0.09	-0.01	-0.25	-0.03	-0.11	-0.22
	Winter	-0.14	-0.21	-0.19	-0.57	-0.23	0.33	0.36

Guangzhou

		$PM_{2.5}$	PM_{10}	CO	SO_2	NO_2	1-h O_3	8-h O_3
WS	Spring	-0.02	0.00	-0.18	-0.07	-0.04	-0.03	0.06
	Summer	-0.44	-0.42	-0.35	-0.59	-0.50	-0.44	-0.36
	Fall	-0.14	-0.23	-0.24	-0.53	-0.46	-0.45	-0.37
	Winter	-0.27	-0.18	-0.09	-0.15	-0.50	-0.41	-0.26
Temp	Spring	-0.48	-0.49	-0.12	-0.02	-0.51	0.19	-0.02
	Summer	0.37	0.48	-0.03	0.34	-0.01	0.67	0.72
	Fall	-0.38	-0.33	-0.39	-0.02	-0.40	0.14	0.10
	Winter	0.32	0.24	0.33	0.19	0.32	0.36	0.26
RH	Spring	-0.38	-0.46	-0.14	-0.16	-0.26	-0.12	-0.32
	Summer	-0.35	-0.37	0.03	-0.18	0.17	-0.66	-0.75
	Fall	-0.43	-0.53	0.12	-0.10	-0.18	-0.23	-0.36
	Winter	-0.25	-0.32	0.00	-0.56	-0.07	-0.37	-0.49

Table 4. Statistical summary for the top and bottom 10% concentrations of $PM_{2.5}$, PM_{10}, and other gases during the entire sampling period (2013/03 – 2014/02). Units: µg/m^3 for $PM_{2.5}$ and PM_{10}; ppb for all other gaseous pollutants. Numbers in the parentheses represent the bottom 10% concentrations.

		$PM_{2.5}$	**PM_{10}**	**CO**	**SO_2**	**NO_2**	**1-h O_3**	**8-h O_3**
Beijing	Average	243.0 (14.2)	247.4 (32.6)	2599.2 (344.7)	27.2 (1.4)	50.4 (10.9)	119.7 (12.6)	99.7 (8.3)
	Min	177.6 (5.4)	193.6 (14.6)	1985.2 (228.8)	21.0 (0.7)	42.6 (4.1)	100.8 (4.3)	88.2 (2.7)
	Max	391.6 (20.6)	408.8 (42.9)	3882.5 (407.7)	45.7 (1.7)	66.6 (13.3)	143.7 (19.5)	114.6 (13.0)
	Count	34 (34)	31 (31)	32 (32)	33 (33)	33 (33)	30 (30)	30 (30)
Shanghai	Average	150.2 (15.5)	188.0 (33.6)	1293.0 (424.0)	18.7 (3.1)	39.9 (8.1)	112.2 (26.1)	92.7 (19.8)
	Min	107.2 (6.2)	140.8 (22.5)	1064.1 (337.7)	14.2 (2.1)	33. 0 (3.3)	92.0 (15.8)	77.4 (11.0)
	Max	363.4 (19.5)	291.1 (39.5)	2152.4 (460.3)	27.3 (3.7)	53.2 (10.1)	149.9 (32.3)	123.3 (24.8)
	Count	33 (33)	31 (31)	32 (32)	33 (33)	33 (33)	32 (32)	32 (32)
Guangzhou	Average	112.1 (16.1)	145.3 (27.8)	1221.2 (591.5)	13.6 (2.8)	45.8 (12.1)	111.9 (18.9)	95.9 (14.3)
	Min	91.5 (8.3)	123.7 (19.1)	1036.8 (484.5)	11.5 (1.1)	38.7 (8.4)	94.6 (9.7)	77.0 (7.0)
	Max	155.6 (20.6)	192.7 (34.8)	2101.9 (629.3)	19.7 (3.8)	60.5 (13.7)	139.4 (22.8)	134.0 (17.6)
	Count	32 (32)	32 (32)	30 (30)	31 (31)	31 (31)	30 (30)	30 (30)

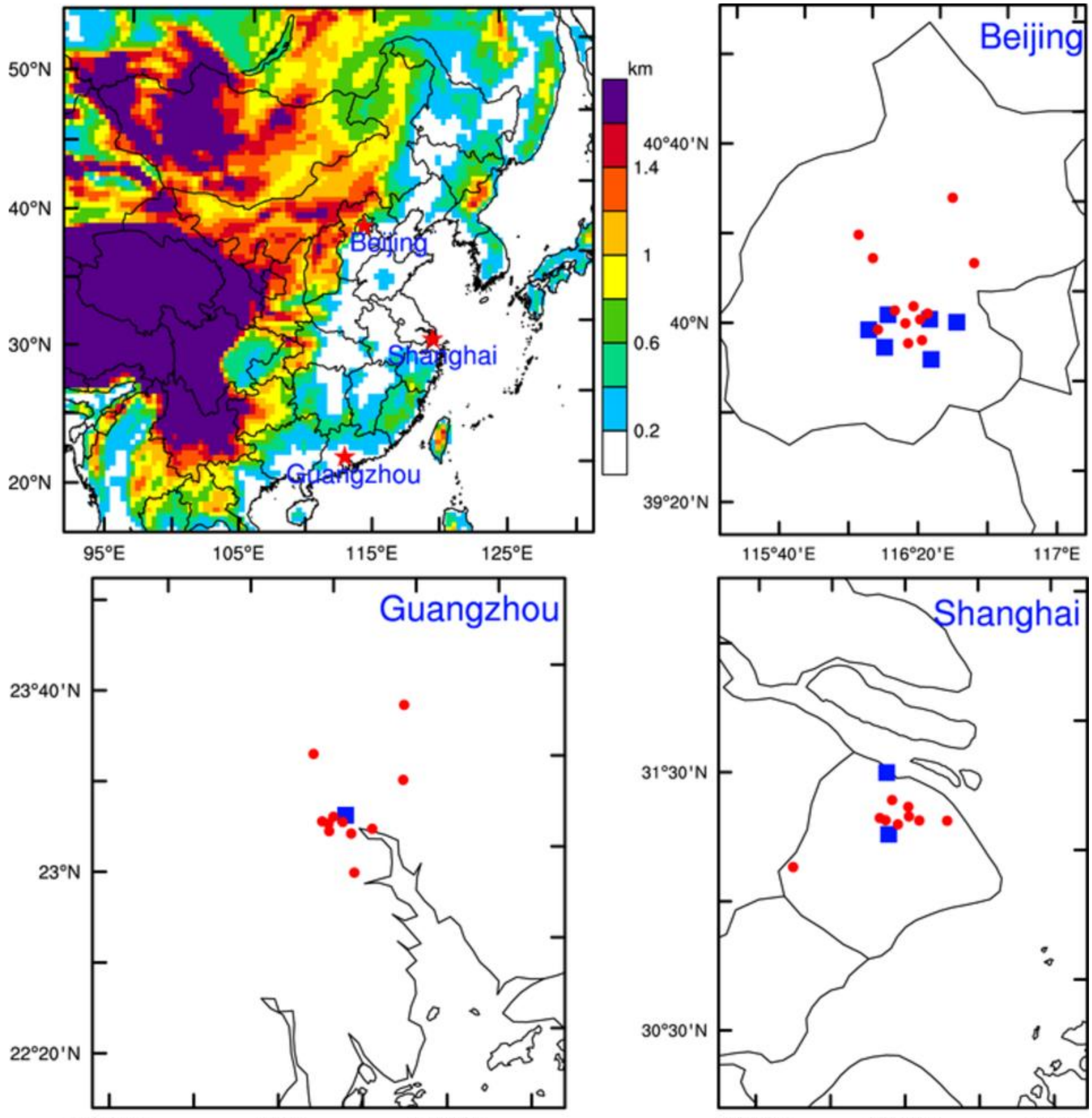

Figure 1. Maps showing the locations of three megacities in China and the locations of meteorological (blue squares) and air quality (red circles) stations in each city.

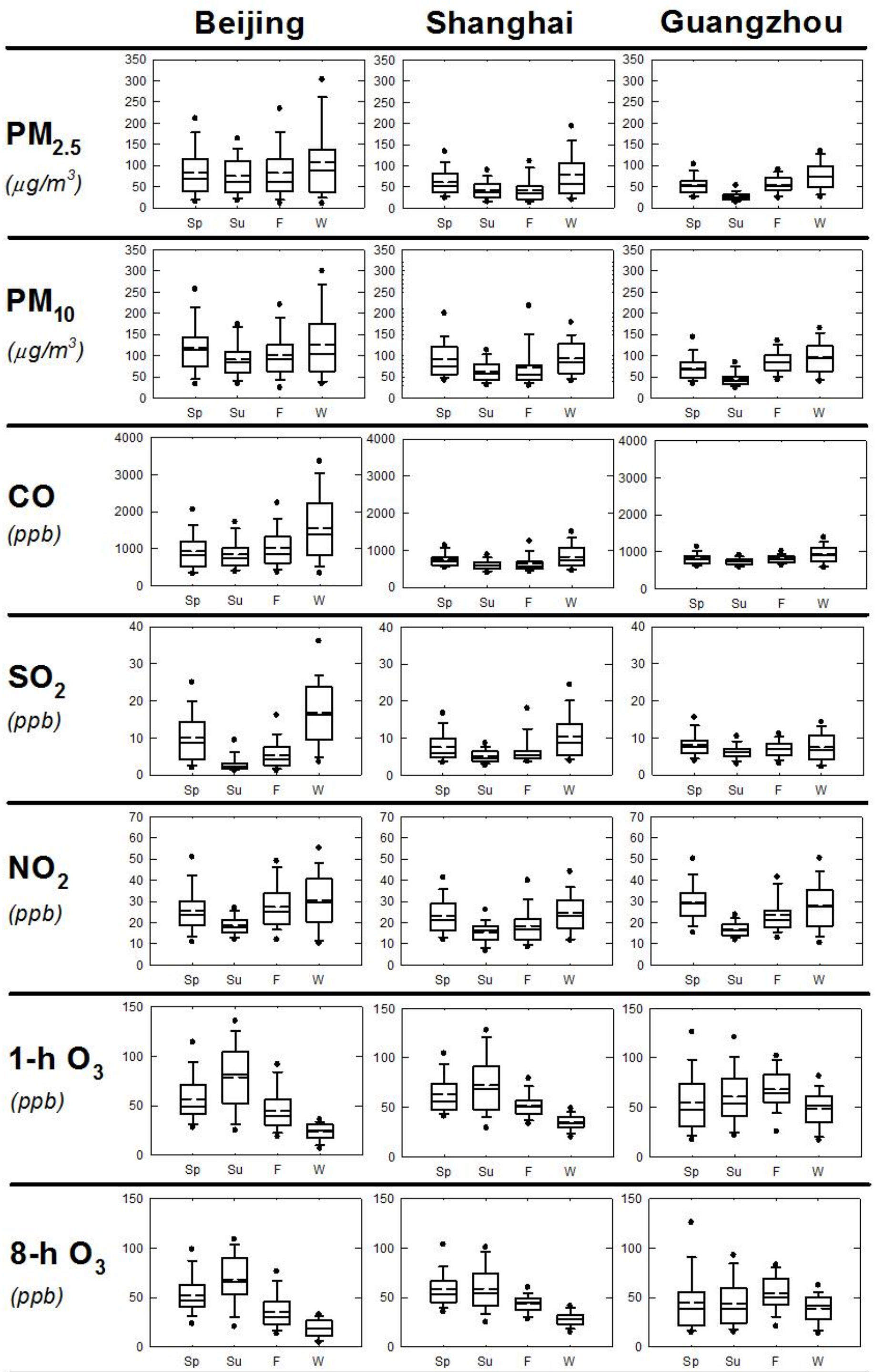

Figure 2. Seasonal variations of criteria air pollutants (Sp, Su, F, and W indicate spring, summer, fall, and winter, respectively). The dash lines represent the arithmetic average. The central box represents the values from the lower to upper quartile (25th to 75th percentile). The vertical line extends from the 10th percentile to the 90th percentile. The middle solid line represents the median. The dash line represents the arithmetic average. Outliers are plotted as dots.

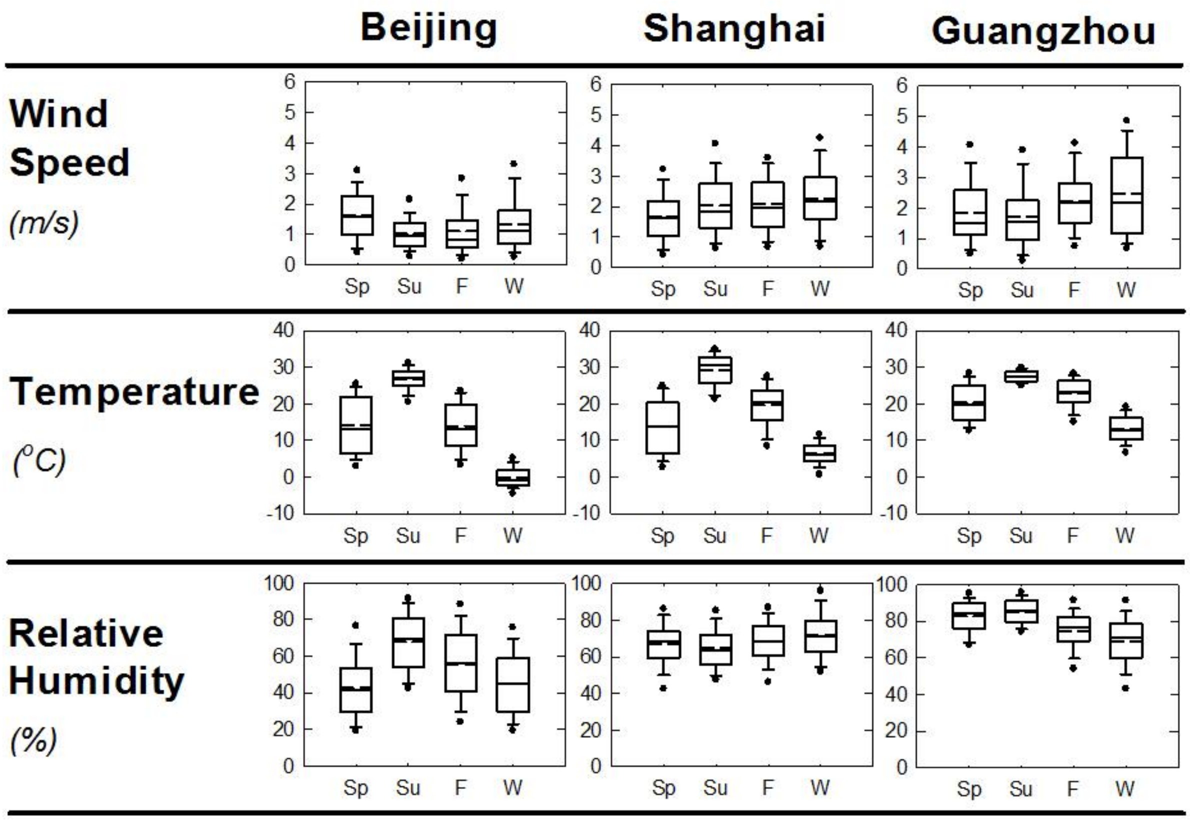

Figure 3. Seasonal variations of wind speed, temperature, and relative humidity (Sp, Su, F, and W indicate spring, summer, fall, and winter, respectively). The central box represents the values from the lower to upper quartile (25th to 75th percentile). The vertical line extends from the 10th percentile to the 90th percentile. The middle solid line represents the median. The dash line represents the arithmetic average. Outliers are plotted as dots.

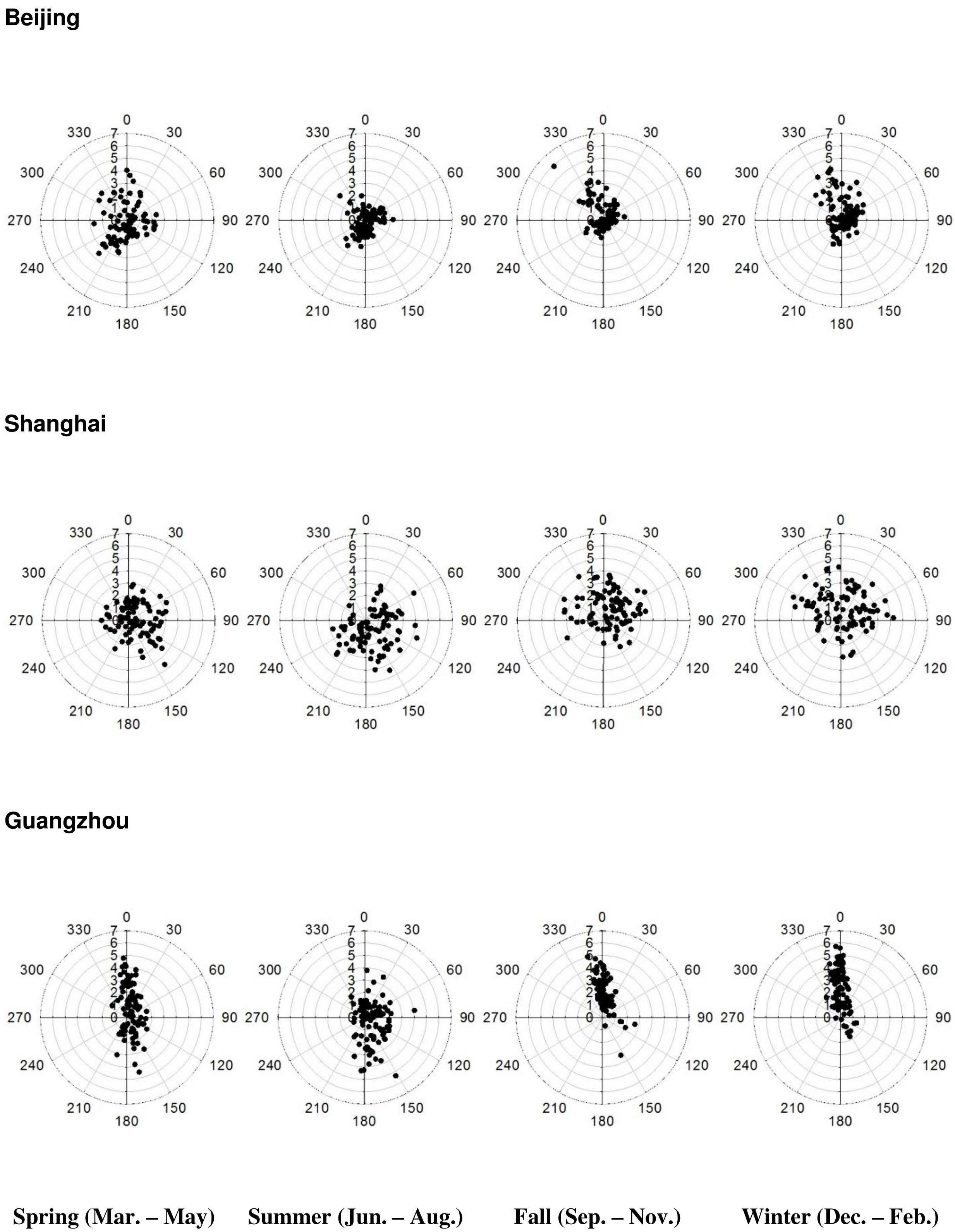

Figure 4. Seasonal records of wind speed (m/s) corresponding with wind direction.

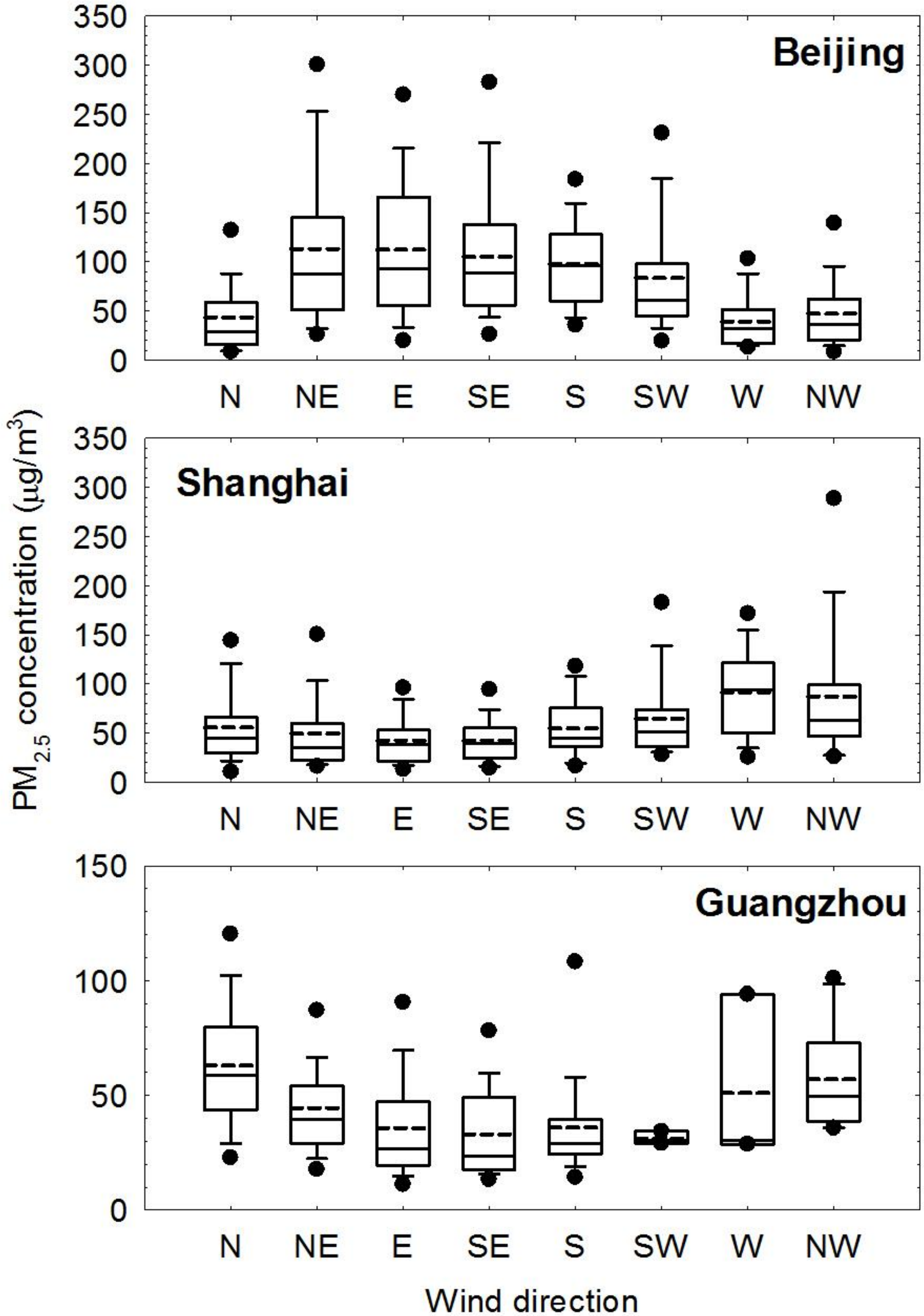

Figure 5. Box-Whiskers plots with the concentrations of $PM_{2.5}$ according to their respective wind directions. PM_{10}, CO, SO_2, NO_2, 1-h O_3 and 8-h O_3 plots are included in supplemental materials (Figure S3).

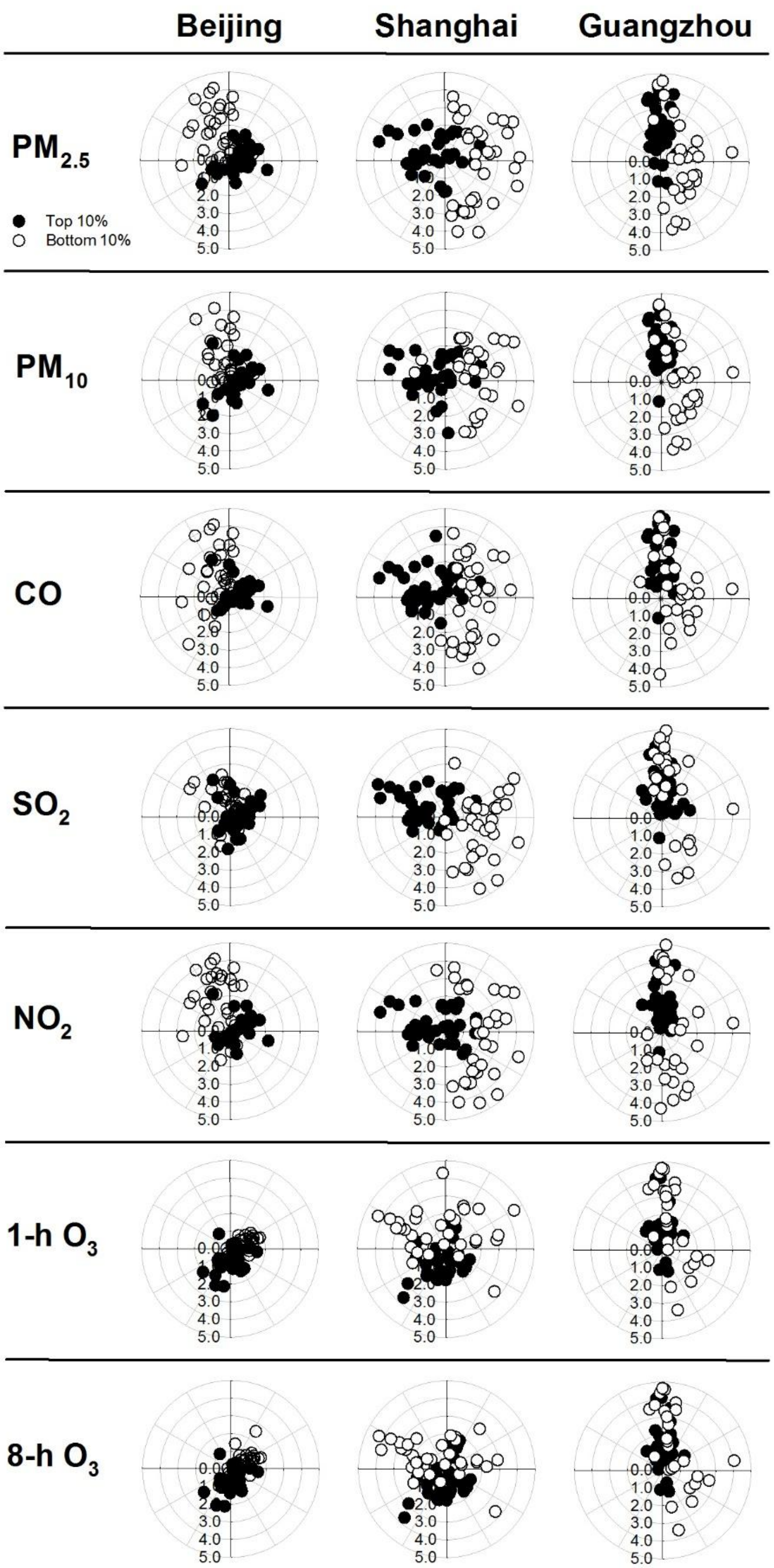

Figure 6. Comparison of wind profiles between top 10% and bottom 10% measurements of pollutants.

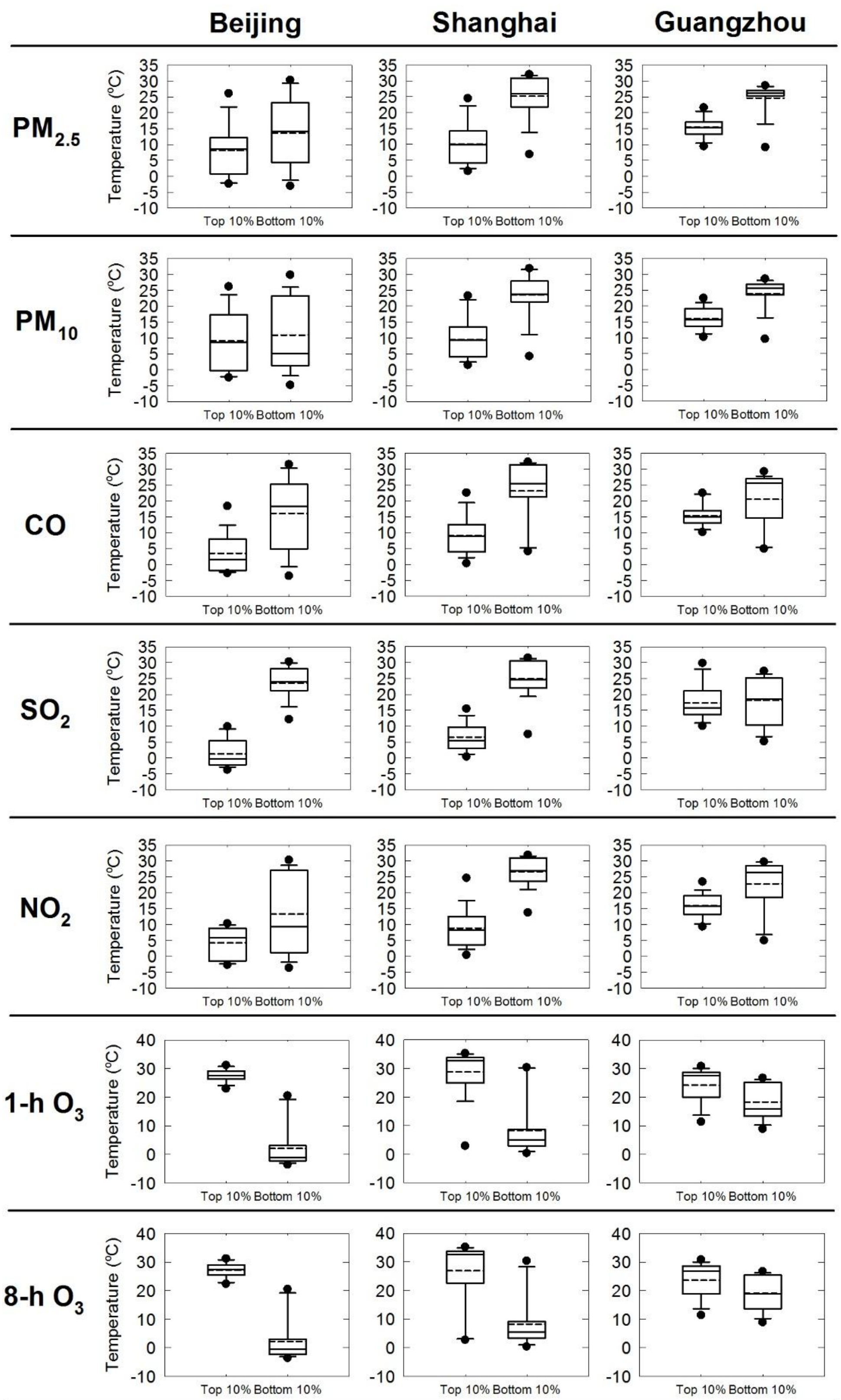

Figure 7. Comparison of temperature profiles between top 10% and bottom 10% pollutant concentrations.

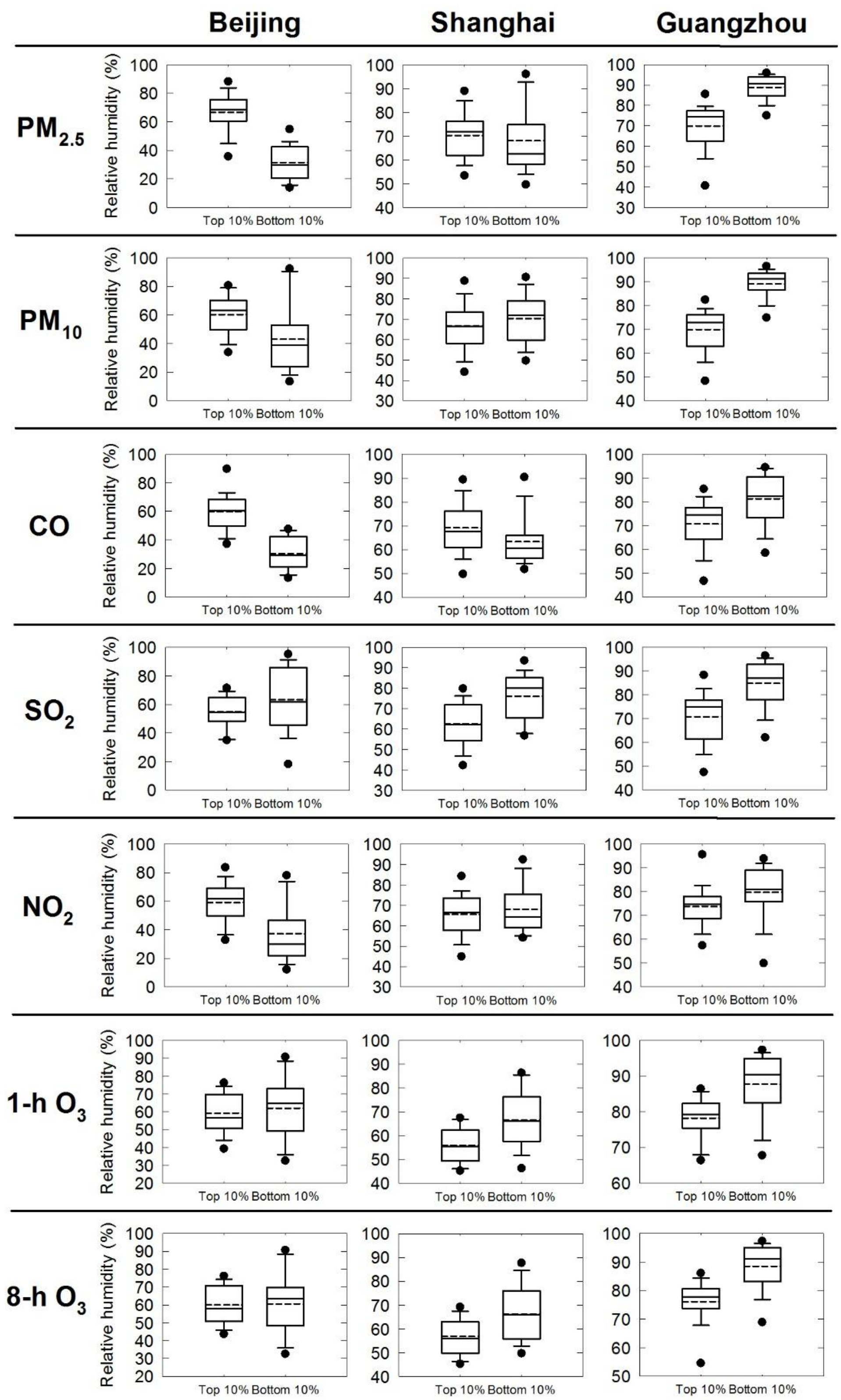

Figure 8. Comparison of relative humidity profiles between top 10% and bottom 10% measurements of pollutants.

Supplemental Materials

Relationships between meteorological parameters and criteria air pollutants in three megacities in China

Hongliang Zhang[1], Yungang Wang[2,*], Jianlin Hu[3], Qi Ying[4], Xiao-Ming Hu[5]

[1]Department of Civil and Environmental Engineering, Louisiana State University, Baton Rouge, LA 70803, USA
[2]Environmental Resources Management (ERM), Walnut Creek, CA 94597, USA
[3]Department of Civil and Environmental Engineering, University of California, Davis, CA 95616, USA
[4]Zachry Department of Civil Engineering, Texas A&M University, College Station, TX 77843, USA
[5]Center for Analysis and Prediction of Storms, and School of Meteorology, University of Oklahoma, Norman, OK 73072, USA

*Corresponding author: Dr. Yungang Wang
Email: carl.wang@erm.com
Telephone: +1-925-946-0455

Table S1. Statistical summary of the daily average atmospheric boundary layer (unit: meter) during March 2013 – January 2014 based on the Weather Research and Forecasting (WRF) simulation.

		Spring	**Summer**	**Fall**	**Winter**
Beijing	Average	938	967	634	415
	Min	206	291	203	117
	Median	869	962	592	364
	Max	2121	1515	1475	1159
	Count	89	92	91	62
Shanghai	Average	540	701	714	568
	Min	146	292	236	209
	Median	524	700	687	563
	Max	900	1160	1419	1151
	Count	89	92	91	62
Guangzhou	Average	657	808	694	544
	Min	278	366	349	292
	Median	678	829	717	545
	Max	1021	1063	1064	746
	Count	89	92	91	62

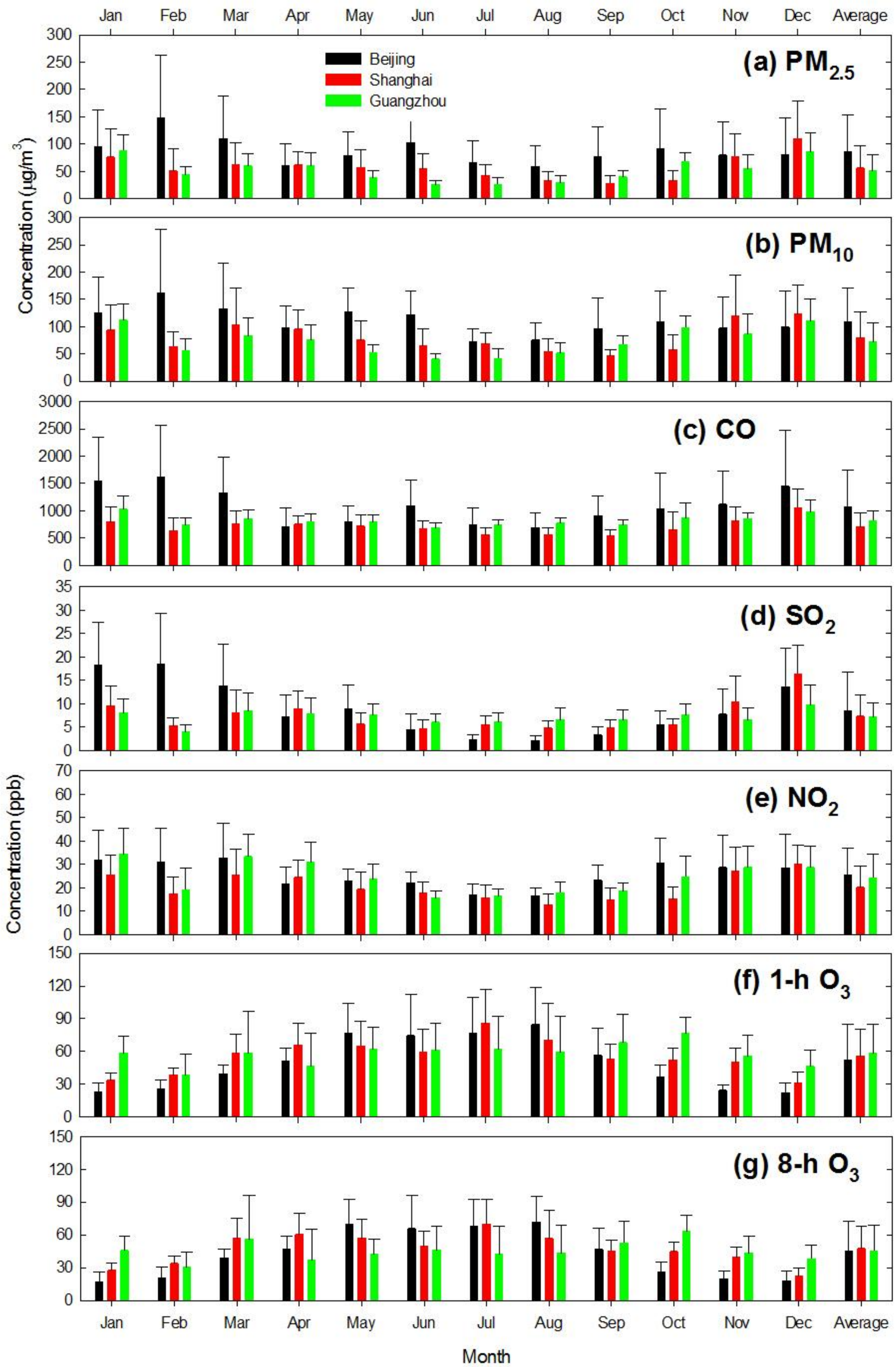

Figure S1. Monthly variations of all pollutants.

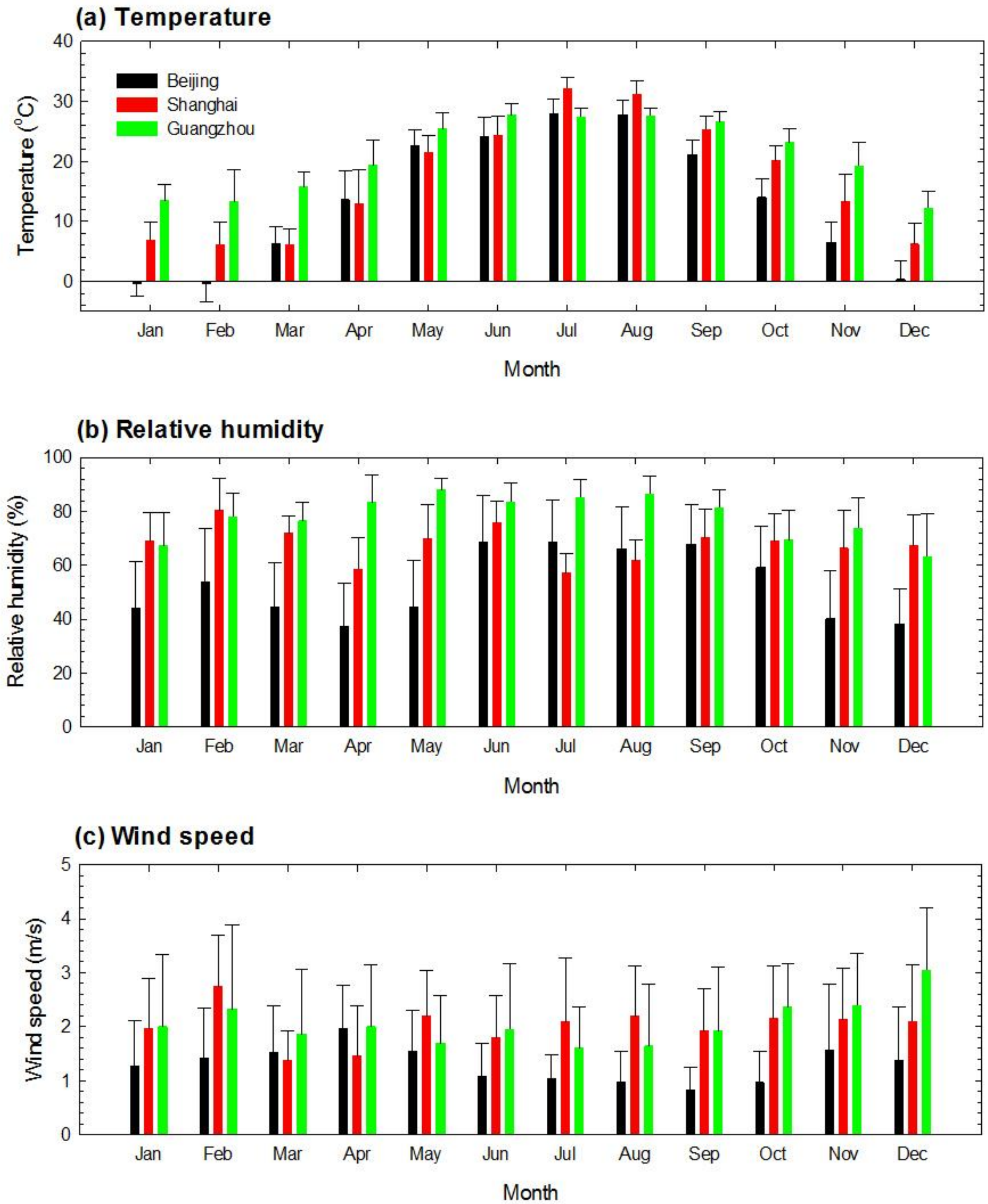

Figure S2. Monthly variations of meteorological parameters.

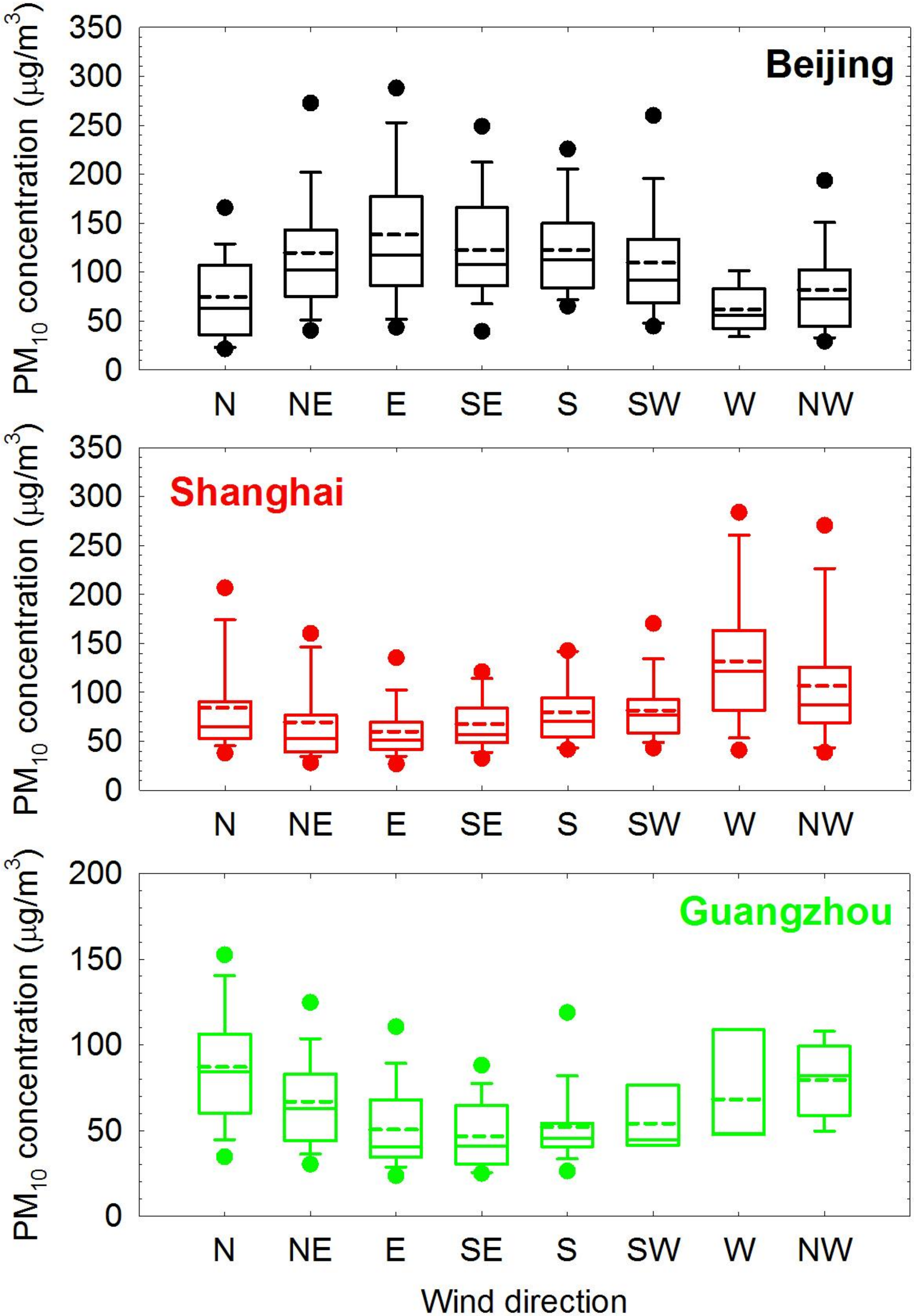
Beijing
Shanghai
Guangzhou
PM10 concentration (µg/m3)
350
300
250
200
150
100
50
0
N
NE
E
SE
S
SW
W
NW
Wind direction

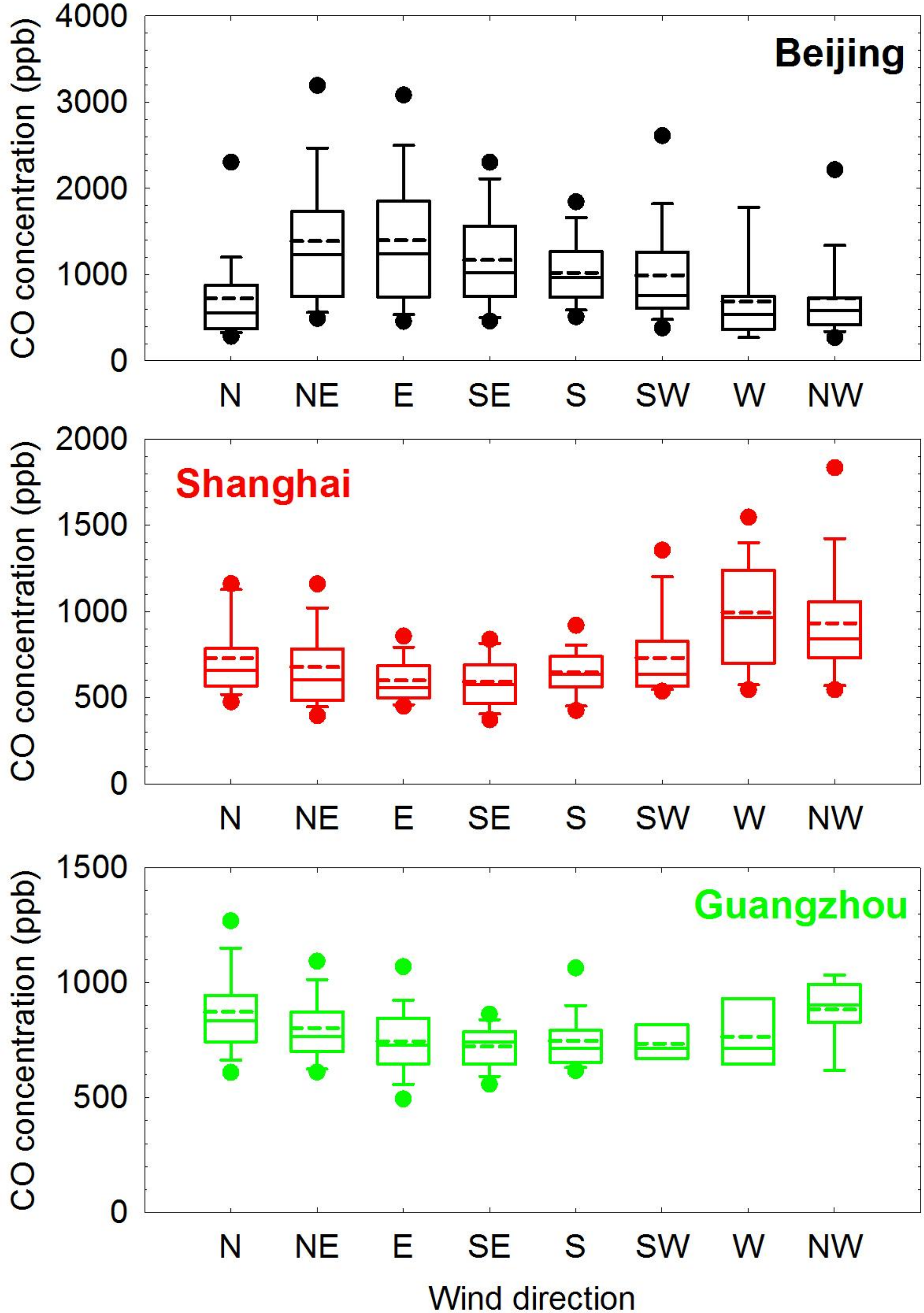
Beijing
CO concentration (ppb)
4000
3000
2000
1000
0
N
NE
E
SE
S
SW
W
NW
Shanghai
CO concentration (ppb)
2000
1500
1000
500
0
N
NE
E
SE
S
SW
W
NW
Guangzhou
CO concentration (ppb)
1500
1000
500
0
N
NE
E
SE
S
SW
W
NW
Wind direction

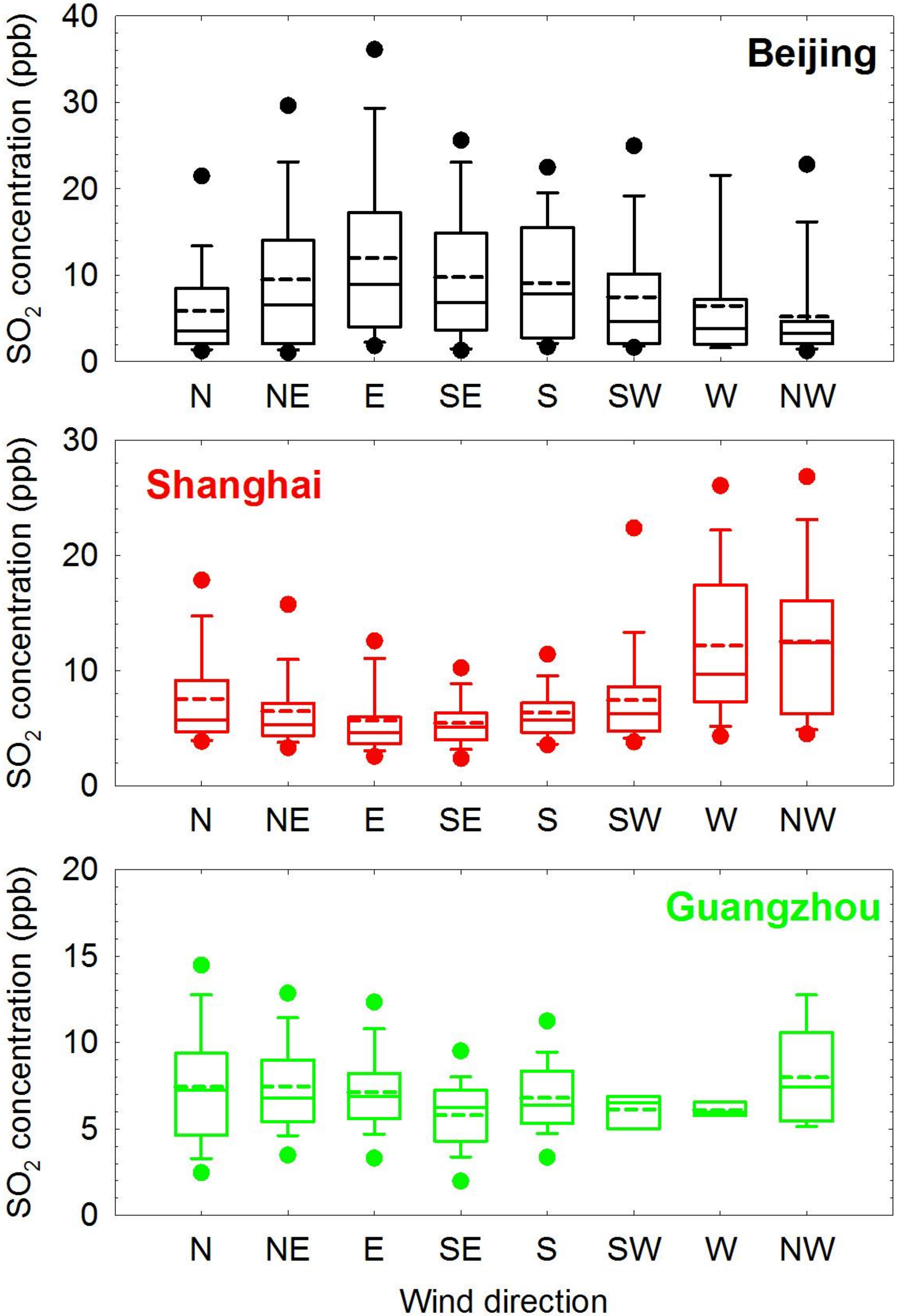

SO2 concentration (ppb)
40
30
20
10
0
Beijing
N
NE
E
SE
S
SW
W
NW
SO2 concentration (ppb)
30
20
10
0
Shanghai
N
NE
E
SE
S
SW
W
NW
SO2 concentration (ppb)
20
15
10
5
0
Guangzhou
N
NE
E
SE
S
SW
W
NW
Wind direction

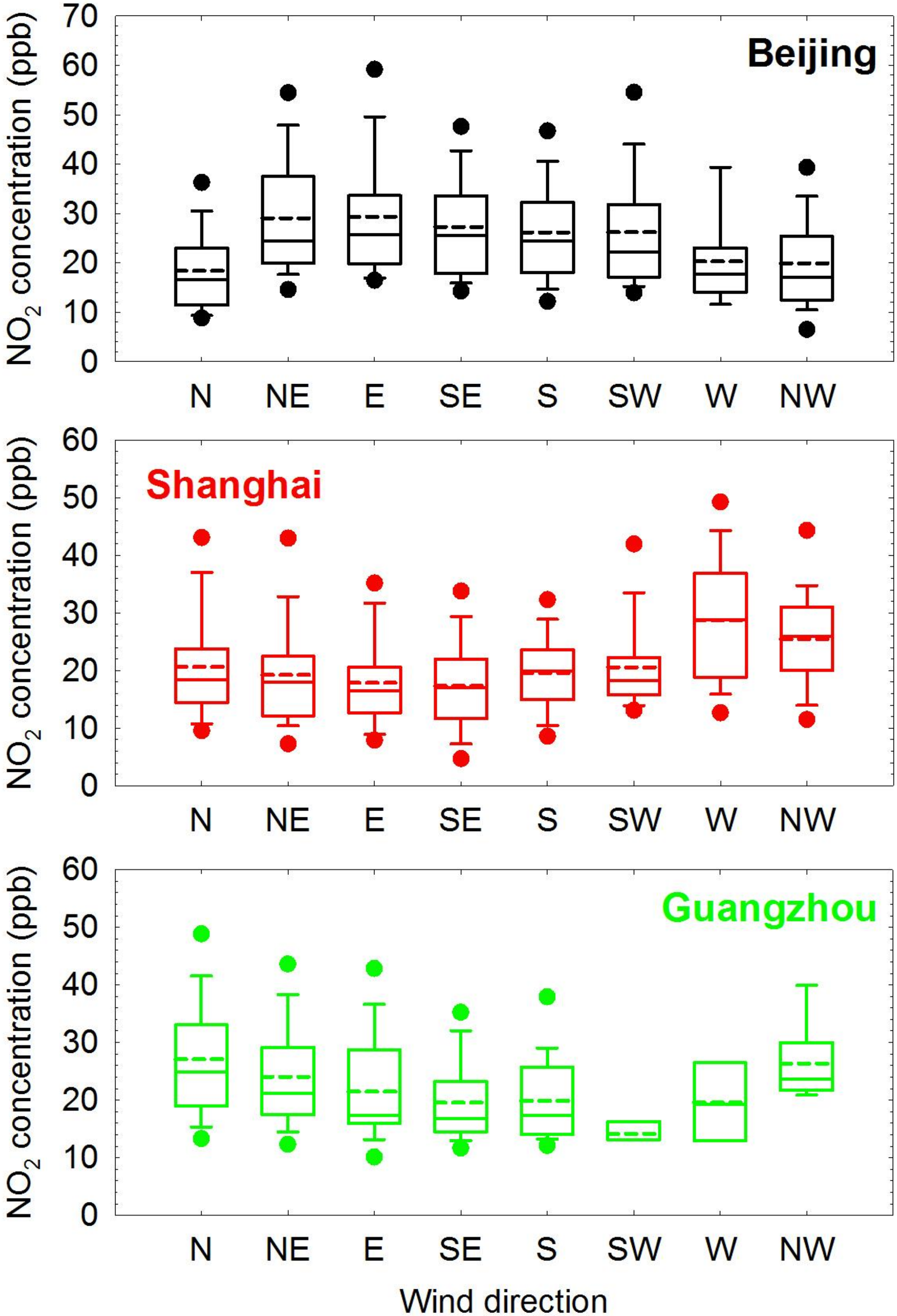
Beijing
Shanghai
Guangzhou
NO_2 concentration (ppb)
N NE E SE S SW W NW
Wind direction

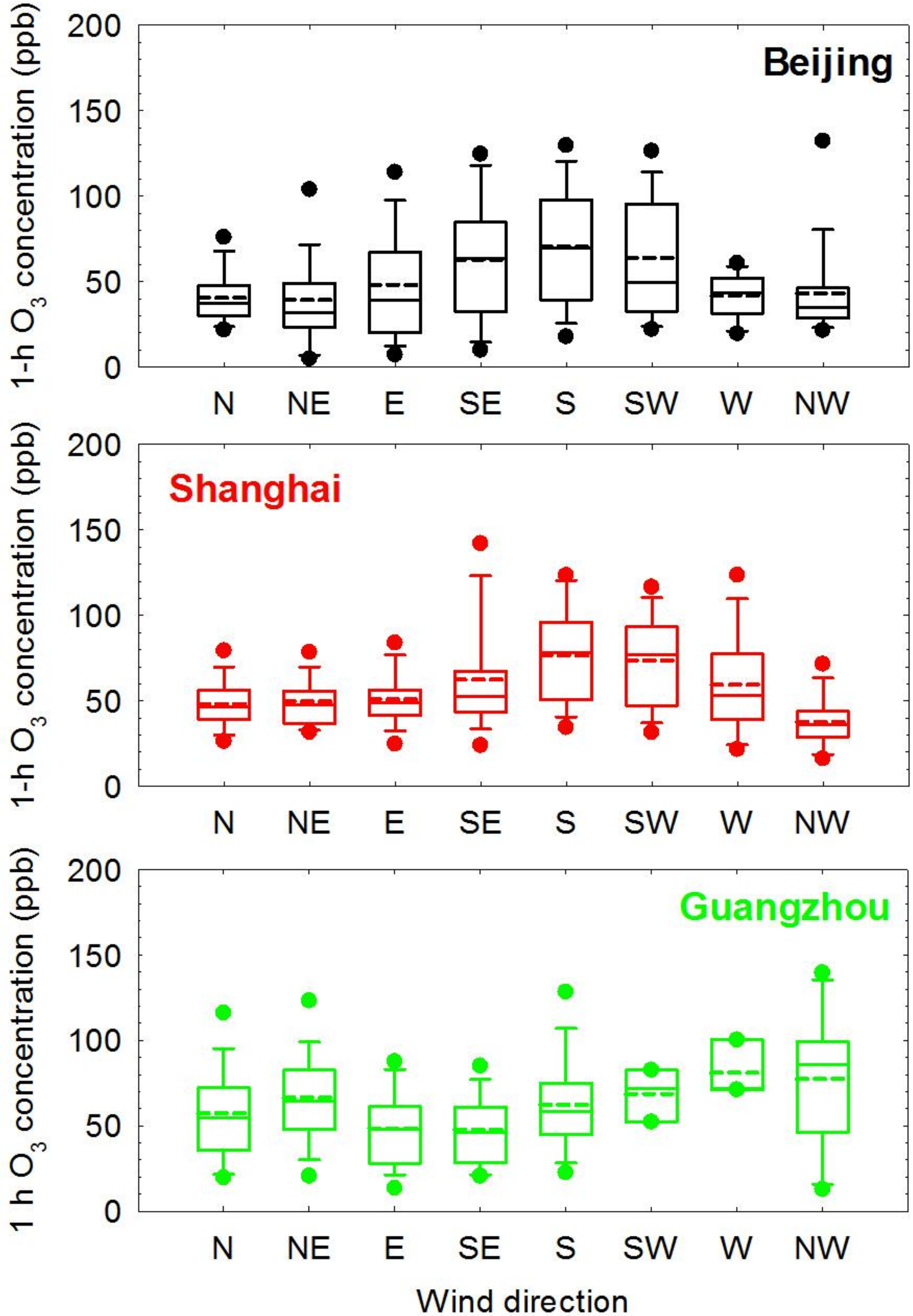
Beijing
Shanghai
Guangzhou
1-h O3 concentration (ppb)
1 h O3 concentration (ppb)
0
50
100
150
200
N
NE
E
SE
S
SW
W
NW
Wind direction

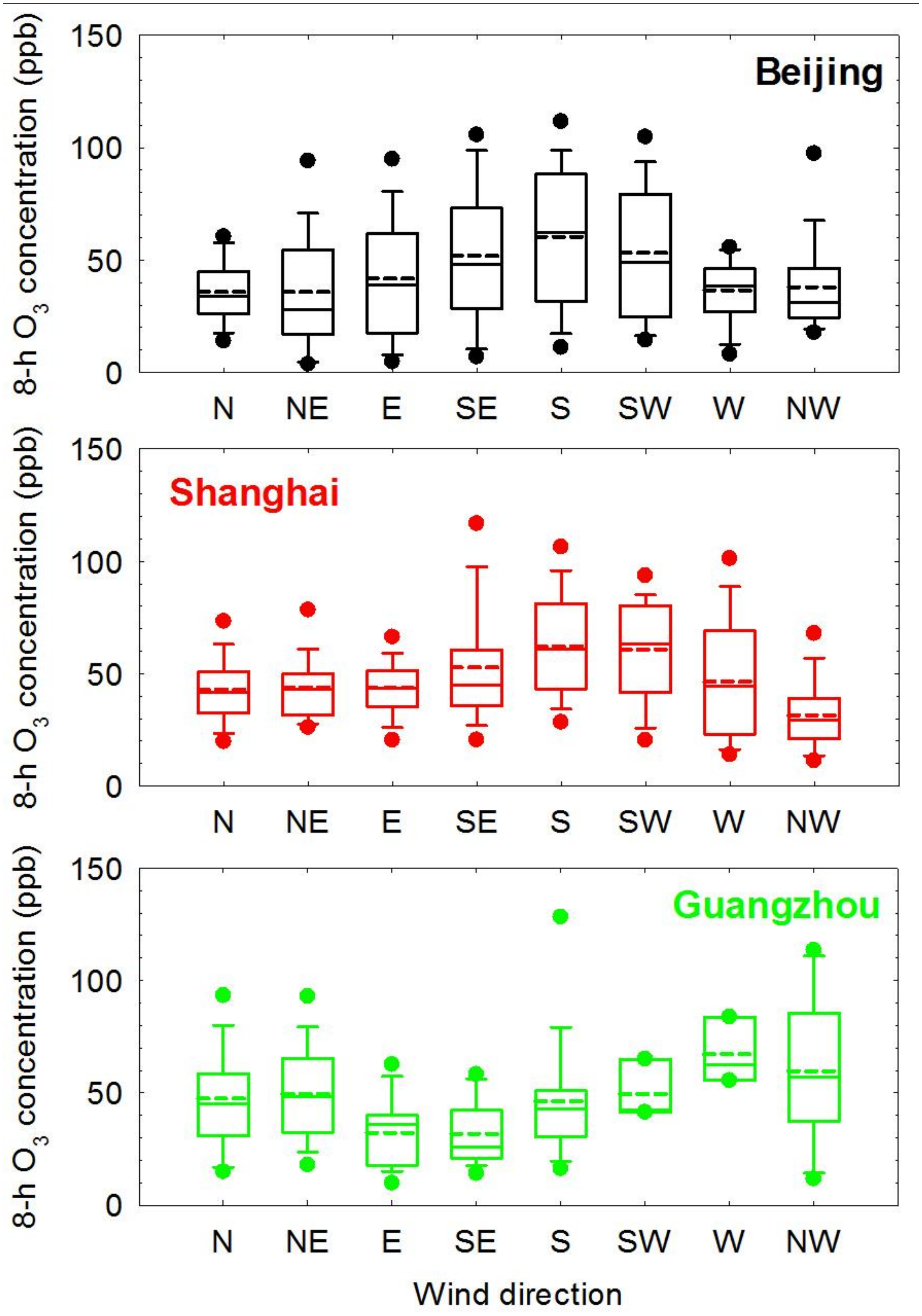

Figure S3. Box-Whiskers plots with the concentrations of PM_{10}, CO, SO_2, NO_2, 1-h O_3 and 8-h O_3 according to their respective wind directions.